ISSN 0276-1084

VOL. 31 NO. 1 MAY 2012

GEO-HEAT CENTER QUARTERLY BULLETIN

GEOTHERMAL USE in the DAKOTAS

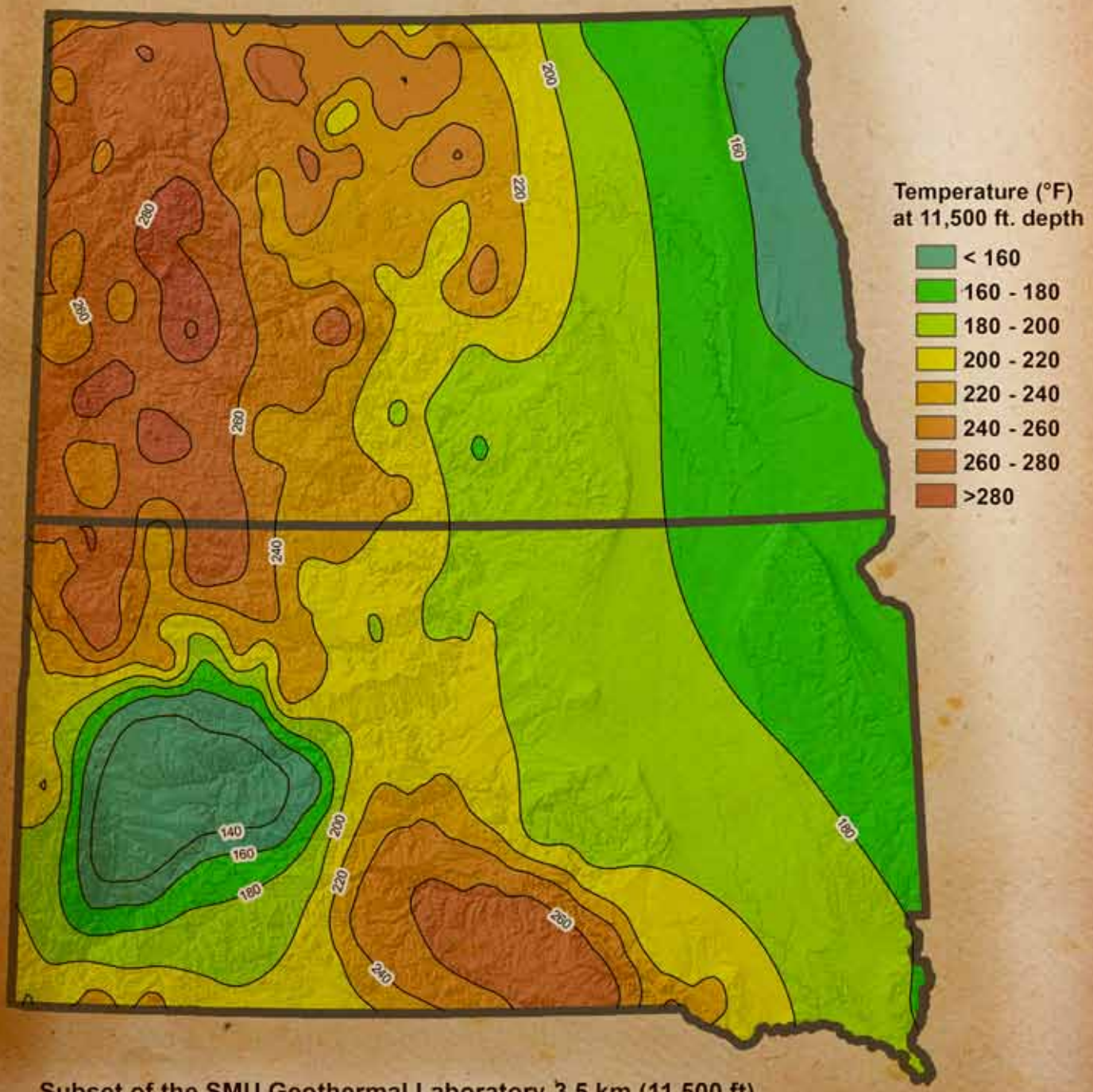

Subset of the SMU Geothermal Laboratory 3.5 km (11,500 ft) Temperature at Depth Map, Blackwell et al., 2011

SMU GEOTHERMAL LABORATORY

OREGON INSTITUTE OF TECHNOLOGY • KLAMATH FALLS, OREGON 97601-8801 • (541) 885-1750

VOL. 31 NO. 1 MAY 2012

GEO-HEAT CENTER QUARTERLY BULLETIN

ISSN 0276-1084

A Quarterly Progress and Development Report on the Direct Utilization of Geothermal Resources

CONTENTS

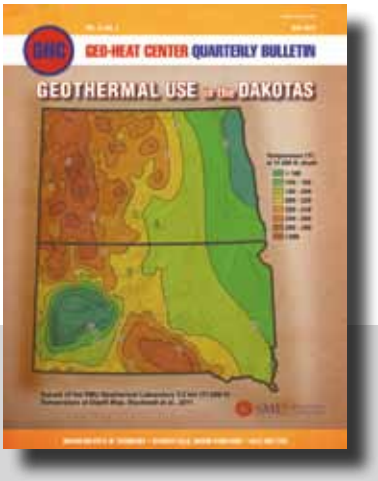

Cover: Temperature-at-Depth Maps for 3.5 to 9.5 km, Google.org/EGS (Blackwell, D.D., M. Richards, Z. Frone, J. Batir, A. Ruzo, R. Dingwall, and M. Williams, 2011).

PUBLISHED BY

GEO-HEAT CENTER
Oregon Institute of Technology
3201 Campus Drive
Klamath Falls, OR 97601
Phone: (541) 885-1750
E-mail: geoheat@oit.edu

All articles for the *Bulletin* are solicited. If you wish to contribute a paper, please contact the editor at the above address.

EDITOR

Tonya "Toni" Boyd
Cover Design – SmithBates Printing & Design

WEBSITE:

http://geoheat.oit.edu

ACKNOWLEDGEMENT

This material is based upon work supported by the Department of Energy (National Nuclear Security Administration) under Award Number DE-EE0002741.

SUBSCRIPTIONS

The *Bulletin* is mailed free of charge. Please send your name and address to the Geo-Heat Center for addition to the mailing list.

If you wish to change your *Bulletin* subscription, please complete the form below and return it to the Geo-Heat Center.

Name _____

Address _____

City, State, Zip _____

Country _____

THE ECONOMIC, ENVIRONMENTAL, AND SOCIAL BENEFITS OF GEOTHERMAL USE IN THE DAKOTAS

Andrew Chiasson, Geo-Heat Center, Oregon Institute of Technology, Klamath Falls, Oregon

North Dakota and South Dakota (the Dakotas) are not normally thought of as geothermal states, but direct uses of geothermal energy have existed for centuries. Today, the documented direct uses of geothermal waters are limited to South Dakota and are related to space and district heating, spas and resorts, and aquaculture. There are also many undocumented individual uses by ranchers, particularly in the winter months for space heating, stock watering, and snow melting. In addition to geothermal direct uses, numerous applications of geothermal heat pumps exist in the Dakotas. Further, the University of North Dakota is currently conducting research on the feasibility of electrical power generation from co-produced fluids (petroleum and hot water) from the deep petroleum wells in the Williston Basin – a deep sedimentary basin extending through western North and South Dakota, eastern Montana, and southern Saskatchewan known for its rich deposits of petroleum.

ECONOMIC BENEFITS

South Dakota has a rich history of use of geothermal waters for medicinal and curative purposes (balneology). Fall River County, in the southwestern corner of the State, is the only place where extensive development of balneology has taken place. Historically, Sioux and Cheyenne Indians frequented the warm and healing waters they called "wiwilakahta," or "hot springs." Tribes considered the soothing springs so important that they waged war over them in the 1840s, and locals now tell of a fierce battle that raged on the east summit above the springs and river (now called Battle Mountain), with the Sioux emerging victorious. When European settler Fred Evans arrived in 1879, he considered the 87°F water a potential moneymaker, envisioning a warm water resort like those back East. Other homesteaders settling the area claimed it eased rheumatism, stomach troubles and other ailments. In 1890, Evans built a dome over several large springs and created Evans Plunge (Figure 1), the world's largest natural warm-water indoor swimming pool, which still exists today in what is now the city of Hot Springs, SD. According to South Dakota Magazine, Evans' venture may have been the unofficial start of the Black Hills' tourism industry, and today, families visiting the Southern Hills usually stop at Evans Plunge for a soak in hot tubs or a ride down one of three water slides into the big pool. From the inflow of 5,000 gallons of water per minute from the springs arising out of the pebble bottom, there is a complete change of water 16 times daily, thus insuring clean, fresh, living water at all times. The 50-ft. by 200-ft. pool ranges in depth from 4 ft. to 6 ft. with two shallow enclosures for children.

Except for Evans Plunge, there is very little balneological geothermal use in southwestern South Dakota today. A combination of lack of interest and belief in the therapeutic use of mineral waters, and corrosion and scaling of pipelines led to the demise of the industry in the 1950's (Lund, 1997). Eight other large springs exist in the area, some of which have had bath houses and sanatoriums in the first half of the 20th century. There are over 80 capped wells and springs in the area, but there appears to be a slow revival of some of these past uses, especially the spa therapy (Lund, 1997).

Figure 1. Post card image of Evans Plunge (right), Mammoth Plunge (center), and Courthouse (left.) circa 1908. Evans Plunge still exists today, but Mammoth Plunge, a large bathhouse, was torn down in the 1960s. (http://usgwarchives.org/sd/fall_riv / postcards/bevhs.jpg).

Other uses of geothermal waters in the Dakota States for balneological purposes occurs at the Stroppel Hotel, located in Midland, SD about 60 miles west of Pierre, SD. The small hotel uses warm water from a well drilled in 1939 to a depth of 1,784 ft., which produces 33 gallons per minute of water at 116°F. The hotel caters to spa guests with three 8-ft. by 8-ft. separately enclosed bath tubs, each filled with 4 ft. of hot mineral water continually flowing through them. The hotel is also heated by the geothermal water.

The greatest use of direct geothermal energy today in the Dakotas is, by far, space and district heating. South Dakota currently has two municipal geothermal district heating systems and one "mini-district" heating system, in addition to many standalone buildings heated directly with geothermal energy.

The Philip, SD district heating project was based on a Program Opportunity Notice (PON) solicitation and the resulting grant of cost shared funds, and the project was completed in 1982 at a cost of $1.21 million (Lund, 1997). The geothermal well is 4,200 ft. deep, producing 340 gallons per minute of 157°F water to heat Haakon School. The geothermal water is then cascaded to heat downtown businesses. Currently, the district system heats five school buildings (total floor area of about 44,000 sq. ft.) of the Haakon School District and eight downtown buildings. With ARRA funds, the Hans P. Peterson Memorial Hospital has been connected to the district heating system, and will

become a customer in 2012. The district system includes a special design to remove Radium-226 from the spent fluid using barium chloride before the water is disposed of in the Bad River.

Philip, SD also has a "mini-district" geothermal heating system, sourced from a geothermal well located about 2.5 miles north of town, just west of Lake Waggoner. The well is owned by the City of Philip, and was drilled in the 1970s to a depth of 5,280 feet, and can produce 700 gallons per minute of water at 157˚F. The district customers have changed over the years, with the system at first supplying heat to the Haakon County highway equipment maintenance shop, a water treatment plant, and a greenhouse operation. Today, the well still provides heat to the Haakon County highway equipment maintenance shop, and the greenhouses, which are now used for an aquaculture operation to raise Tilapia for commercial markets. The water treatment plant is no longer in existence, as Philip obtains drinking water from another source. However, the well now provides heat to the adjacent golf course club house and a small private business. The well is artesian, and spent water is used as irrigation water on the golf course. This well also serves as a community heating well for ranchers who come and load up hot water for various ranching needs, including hot water washing, ice thawing, and snow melting (VanLint, 2012).

The Midland, SD district heating system uses a municipal well drilled in 1969 to a depth of 3,300 ft. that supplies 152˚F water at over 180 gallons per minute (Lund, 1997). The well supplies hot water to heat approximately 40,000 sq. ft. of floor space, including two school buildings, a church, campground buildings and pool, car wash, four downtown buildings, and about 12 residential buildings that were added to the district system around 2002 (Nemec, 2012). Some of the water from the supply well is treated and supplied to the town for domestic water use, while used geothermal water is discharged into a creek and the Bad River. In addition, there is a hot water valve at the well where ranchers can obtain hot water for their stock watering tanks in the winter, and highway maintenance personnel and ranchers clean their equipment in the summer.

The Dakotas also have a history of large single-building uses of space heating. St. Mary's Hospital in Pierre, SD received a PON grant to drill a geothermal well (Lund, 1997), and completed a 2,200-ft. deep well in 1980. The well produced 375 gallons per minute of water at 106˚F that was used to heat portions of the hospital up until recently in 2004, when a hospital expansion resulted in the geothermal well to be taken out of service.

Another large use of geothermal space heating is at Scotchman Industries (Figure 2), which is an 80,000 sq. ft. manufacturing facility in Philip, SD. Scotchman Industries is a leading producer of metal fabricating equipment, accessories, and custom tools, which began in the early 1960's by making and selling farm-related products, such as pickup stock racks, corral panels, gates and chutes. The facility has been heated with geothermal energy since the 1970s from a 2,400-ft. deep well producing water at 110˚F (Kroetch, 2012).

Figure 2. Aerial photo of Scotchman Industries, Philip, SD (http://www.scotchman.com/about/).

The numerous geothermal-related businesses across the Dakotas employ many people directly and indirectly. Geothermal heating systems are generally low-maintenance, and therefore employ only a few folks that are qualified to work on them. In fact, folks in Midland, SD remark that the district geothermal heating system practically runs itself. However, space heating of buildings and other applications using geothermal energy for heat results in significant energy cost savings to people, which, in turn, results in money that can be kept in the local economy. Relative to 2011-2012 natural gas prices, an estimated $1.3 million is saved annually by South Dakotans using geothermal energy, representing dollars that can stay in the local economy. The use of geothermal energy that directly employs the most people in the Dakotas is related to space heating. Some businesses would not exist where they are in South Dakota without the geothermal resource. Mineral spas and resorts (i.e. Evans Plunge) create many direct and indirect jobs in the tourism industry. Using a standard multiplier of 2.5, geothermal businesses create an estimated 100 direct, indirect, and induced jobs in the Dakota States.

ENVIRONMENTAL BENEFITS

In addition to energy savings, geothermal energy usage prevents the emissions of greenhouse gases (GHG) and air pollutants, helping to keep a healthy living environment. If these businesses and residences used fossil fuels to generate the heat that geothermal water provides, they would emit at least 27,679 tonnes of carbon dioxide equivalent each year (Table 1) — the equivalent of removing 5,411 passenger vehicles from the road, saving 64,371 barrels of oil, and saving 5,890 acres of pine forest.

SOCIAL BENEFITS

Social benefits are difficult to measure quantitatively. One key social benefit from geothermal energy use in South Dakota, however, is improved quality of life through recreation and spa therapy. District energy systems are known to promote and foster community pride. Geothermal sources provide many unique recreational opportunities enjoyed by

tens of thousands of people each year, attracting tourists to the state. Given the rich history of the geothermal spa industry, social benefits have been evident for many past generations. According to South Dakota Magazine, Evans Plunge in the 1890s may have been the unofficial start of the Black Hills' tourism industry.

THE FUTURE

The Dakotas have significant geothermal potential for future uses, from new and expanding applications of direct use heating, to resurgence in mineral spa therapy, to development of low-to-moderate temperature resources for electrical power generation. In addition, geothermal heat pump installations continue to grow, with over 1,100 installations now in North Dakota alone (Manz, 2012). Mitchell, SD is home to Hydron Module, a geothermal heat pump manufacturer now operating in an 80,000 sq. ft. facility, making quality products since 1989.

The Geo-Heat Center lists over 50 communities in the Dakotas that are within 5 miles of a geothermal resource with a temperature of 122°F or greater, making them possible candidates for district heating or other geothermal use. South Dakota has a rich history related to the use of mineral waters for medicinal purposes, a practice which is making a comeback.

Researchers at the University of North Dakota continue to explore electrical power generation from co-produced fluids from the Williston Basin in North Dakota. The Williston Basin has been extensively drilled for petroleum production, with over 19,000 wells in North Dakota alone. Wells in the western part of the State record bottom hole temperatures favorable for electrical power production and/or direct use applications.

ACKNOWLEDGEMENTS

This material is based upon work supported by the Department of Energy under Award Number DE-EE0002741.

DISCLAIMER

REFERENCES

Kroetch, J., 2012. Personal communication, J. Kroetch, Scotchman Industries, Philip, SD

Lund, J. W., 1997. "South Dakota Geothermal Resources", *Geo-Heat Center Quarterly Bulletin*, Vol. 18, No. 4, pp. 6-11, Klamath Falls, OR.

Lund, J.W., Freeston, D.H., and Boyd, T.L., 2010. *Direct Utilization of Geothermal Energy.*

Manz, L., 2012. "Geothermal Update", *Geo News.*

Nemec, J., 2012. Personal communication, J. Nemec, former Mayor of Midland, SD.

VanLint, M., 2012. Personal communication, M. VanLint, City Finance Officer, Philip, SD.

Table 1. Energy Production and Carbon Emissions Offsets by Geothermal Energy Utilization in the Dakotas.

Site	Location	Application	Temp.	Annual Energy Use		Annual Emission Offsets (metric tonnes)**		
			(°F)	(10^9 Btu/yr)	(10^6 kWh)	NO_x	SO_x	CO_2
Aquaculture Operation	Phillip, SD	Aquaculture	157	42	12.3	19.1	20.2	11,396
Midland District Heat	Midland, SD	District Heating	152	1.7	0.5	0.8	0.8	451
Philip District Heating (2 sites)	Philip, SD	District Heating	155	18.6	5.4	8.4	8.9	5,033
Evans Plunge	Hot Springs, SD	Resort/Pool	87	36.2	10.6	16.5	17.4	9,822
Scotchman Industries	Phillip, SD	Space Heating	110	3.6	1.1	1.6	1.7	977
Totals				**102**	**30**	**46**	**49**	**27,679**

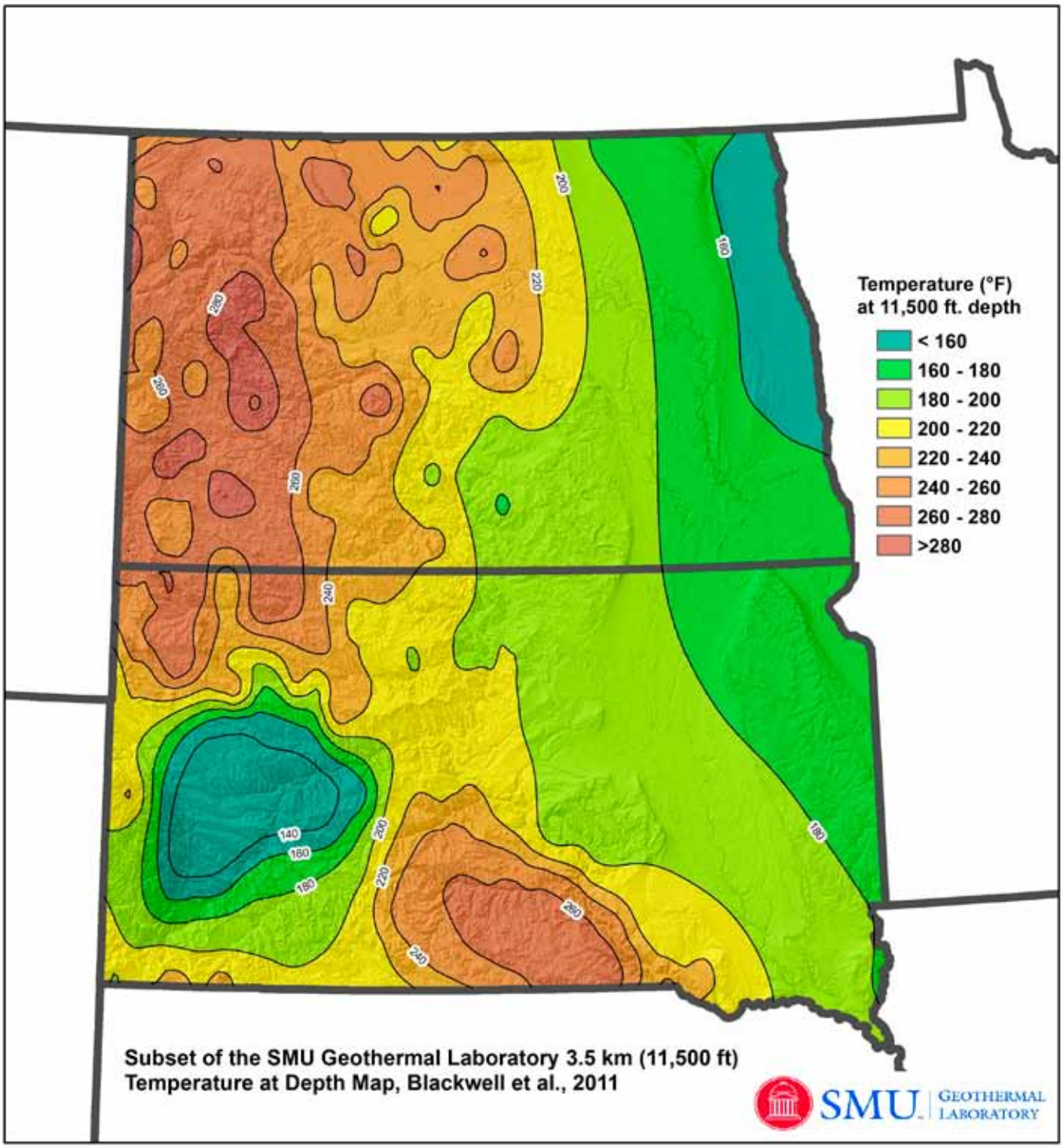

Figure 3. Temperature-at-Depth Maps for 3.5 to 9.5 km, Google.org/EGS (Blackwell, D.D., M. Richards, Z. Frone, J. Batir, A. Ruzo, R. Dingwall, and M. Williams, 2011).

MODELING THE THERMAL EFFECTS OF GROUND SOURCE HEAT EXCHANGE AT STANFORD UNIVERSITY: A PRELIMINARY STUDY

Morgan Ames, Department of Energy Resources Engineering, Stanford University, Stanford, California
Roland N. Horne, Department of Energy Resources Engineering, Stanford University, Stanford, California

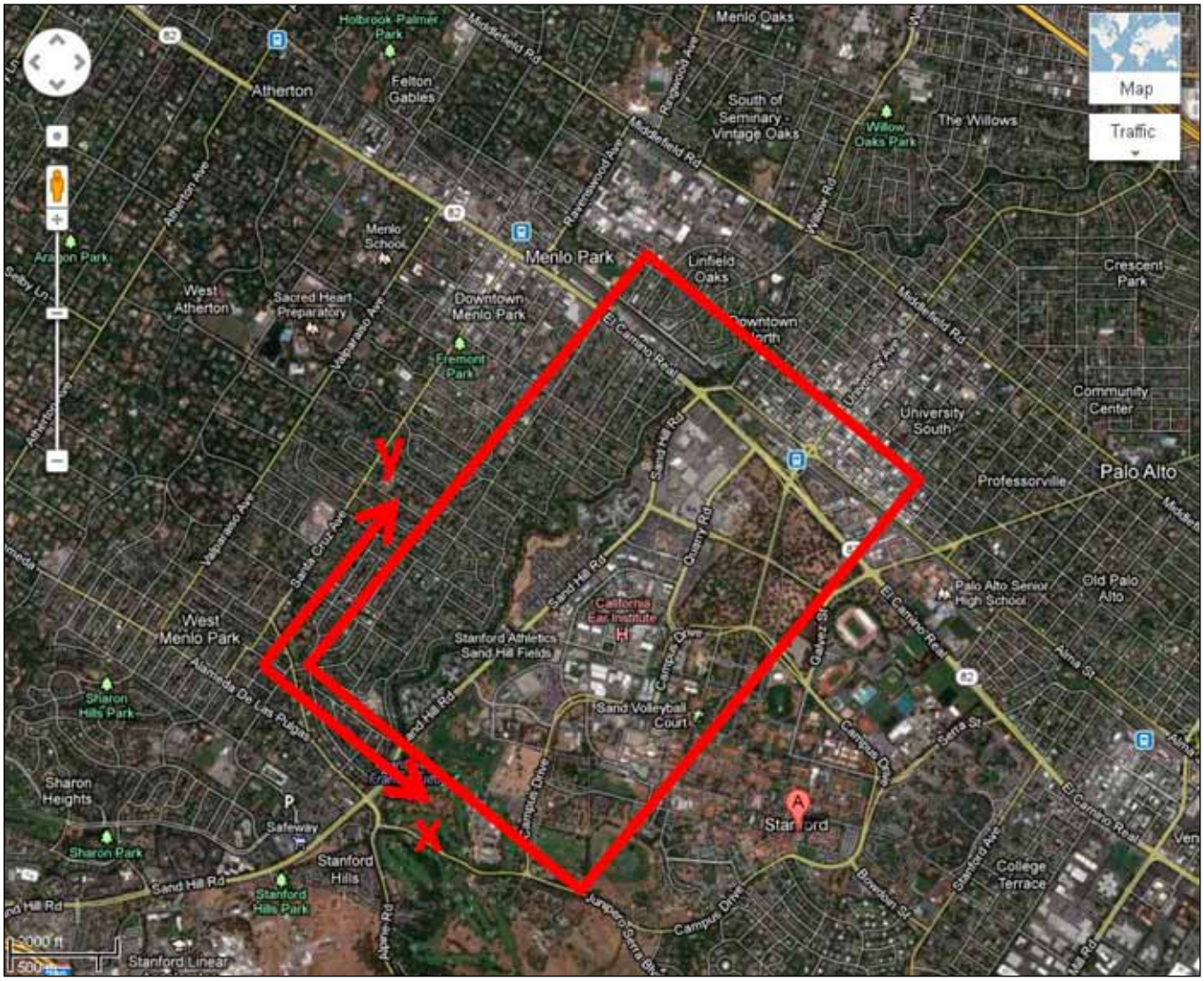

Figure 1: Approximate geographic location of GSHE model (Google maps).

ABSTRACT

The possibility of implementing an open-loop Ground Source Heat Exchanger (GSHE) for heating and cooling on the Stanford University campus is currently being investigated. As part of this preliminary investigation, modeling was performed to estimate the thermal effects of GSHE operation for a hypothetical heating and cooling scheme and well layout. It was found that groundwater temperature in the model experience a small increase due to imbalanced heating and cooling loads after 30 years of operation. However, the thermal plume remains near the GSHE wells after 30 years.

INTRODUCTION

An open-loop Ground Source Heat Exchanger (GSHE) could be used to meet a portion of Stanford University's heating and cooling needs. Analysis is being performed to address the feasibility of GSHE implementation for both heating and cooling on the Stanford University campus.

One concern that affects the feasibility of such a system is its possible impact on groundwater temperature. In order to address this concern, numerical simulation of mass and heat transport was carried out for a hypothetical GSHE scenario described by Luhdorff & Scalmanini Consulting Engineers (2011). The work described here is a first pass at determining the thermal effects of GSHE operation and should be viewed as preliminary analysis.

METHODS

Numerical simulation of single-phase transport of groundwater and of heat transport was carried out. TOUGH2

software was used to model a hypothetical GSHE scenario and estimate its impact on groundwater temperature (Pruess et al., 1999). The software PetraSim was used as an interface for TOUGH2 (Thunderhead Engineering, 2007). This scenario is described here, including a summary of the most important model parameters and assumptions.

The spatial dimensions of the model are provided in Table 1.

Table 1: Basic structure of model.

Model Dimension	Value
Depth at top of model	23 m
L_x	2000 m
L_y	3000 m
L_z	184 m
NX	44 elements
NY	66 elements
NZ	8 elements

These dimensions were chosen based on the hypothetical well layout in the modeled scenario (Luhdorff & Scalmanini, 2011). The depth of 23 m that was used to define the top of the model corresponds to the depth of the water table (Luhdorff & Scalmanini, 2011).

The rock properties used in the model are given in Table 2.

Table 2: Rock properties used in model.

Rock Property	Value
Lateral permeability	55 darcy
Vertical permeability	5.5 darcy
Porosity	20%
Density	2600 kg/m^3
Thermal conductivity	1.7 W/m-°C
Specific heat capacity	872 J/kg-°C

As detailed geological information was lacking for the modeled location, these properties were taken to be homogeneous throughout the model for this initial analysis. Values of rock porosity, permeability, and density were based on estimates provided by Tom Elson of Luhdorff & Scalmanini Consulting Engineers (2011). While a range of permeability values (30 to 55 darcy) and porosity values (20 to 25%) were provided, the high value of permeability and low value of porosity were used such that the flux velocity of the fluid in the aquifer (and thus the velocity of the thermal front in the aquifer) would be the highest value obtainable from these estimates. Thus, the case considered here is intended to be a conservative estimate with regards to thermal interference in neighboring wells. However, it is important to keep in mind that heterogeneity of the flow properties in the aquifer could lead to a much different result than this simple homogeneous case.

Values of rock thermal conductivity and specific heat capacity were based on estimates provided by Haley & Aldrich (2010).

The approximate geographic location of the model is shown in Figure 1. These model boundaries were chosen based on the hypothetical well layout in the modeled scenario as well as the locations of existing neighboring groundwater wells downstream of the GSHE. The hypothetical well layout used in the model is given in Figure 2.

An approximation of natural regional groundwater flow was included in the model. Under present-day conditions, the natural regional groundwater flow direction is northeast, originating in the coastal hills and discharging in the San Francisco Bay (Luhdorff & Scalmanini, 2011). The flow direction in the model was taken to be parallel to the y-axis (see Figure 1). The total rate of natural groundwater flow into and out of the segment of the aquifer of interest in the GSHE scenario was estimated to be between 400 and 800 acre-ft/yr by Luhdorff & Scalmanini Consulting Engineers based on transmissivity estimates and published gradient values (2011). The midpoint of this range was used in the model and was converted to a mass flow rate of 31.3 kg/s using a water density of 1000 kg/m^3.

Regional groundwater flow was assumed to be distributed homogeneously with respect to depth. In other words, each gridblock on the southwestern face of the model was given an equal portion of the total mass flowrate (and correspondingly so for the northeastern face of the model). Finally the temperature of the groundwater flowing into the southwestern face of the model was given a value of 17.78°C, which is based on an estimate provided by Haley & Aldrich (2010).

The initial temperature distribution was assumed to be homogeneous with a value of 17.78°C (Haley & Aldrich, 2010). The initial pressure gradient was assumed to be hydrostatic. The initial value of confining pressure at the top of the model used in the natural state simulation was 311 kPa. This estimate was provided by Casey Meirovitz of Luhdorff & Scalmanini Consulting Engineers and was based on pressures in wells on the Stanford University campus which were measured at the depth of interest (2011).

The well configuration in the hypothetical GSHE scenario includes 8 producers and 18 injectors with flow rates scaled so that the injection and production rates at any given time are equal. (Luhdorff & Scalmanini, 2011). All wells in the model were vertical and specified to allow flow at depths from 46 – 92 m, which was as close to the depths of 150 – 300 ft specified by Luhdorff & Scalmanini Consulting Engineers as discretization allowed (2011). The locations of injection and production wells in this scenario were chosen for high expected well yields as supported by aquifer test data (Luhdorff & Scalmanini, 2011).

The average monthly groundwater production flow rates and reinjection temperatures for the scenario considered are shown in Figure 3 (2011). These values were output from the

Stanford University Central Energy Plant Optimization Model (CEPOM) (2011). The figure also specifies which months correspond to the heating season (October – April) and the cooling season (May – September). These flow rates represent the total production rates of the well field. They are based on expected heating and cooling requirements and the maximum expected production yield for this well configuration as determined by aquifer test data and data from existing wells on the Stanford University campus (Luhdorff & Scalmanini, 2011).

RESULTS

The temperature distribution in the reservoir at different stages of GSHE operation is illustrated in Figures 4 – 6. It is apparent that some heating of the aquifer occurs, with local temperature increases of up to 2.3°C after 30 years of operation. While the spatial extent of the thermal plume increases with time, the heated region remains relatively close to the GSHE wells after 30 years of operation.

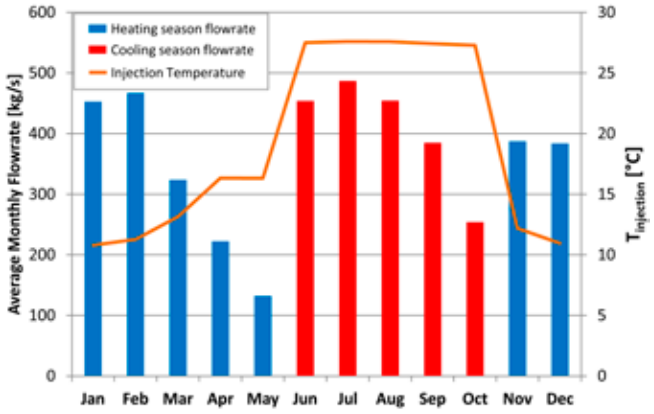

Figure 3: Average monthly GSHE (A) temperatures and (B) flow rates (Luhdorff & Scalmanini, 2011).

The overall heating of the aquifer near the wells is likely a result of imbalanced heating and cooling loads: there is a net heat addition into the aquifer of approximately 4.3 TJ for a

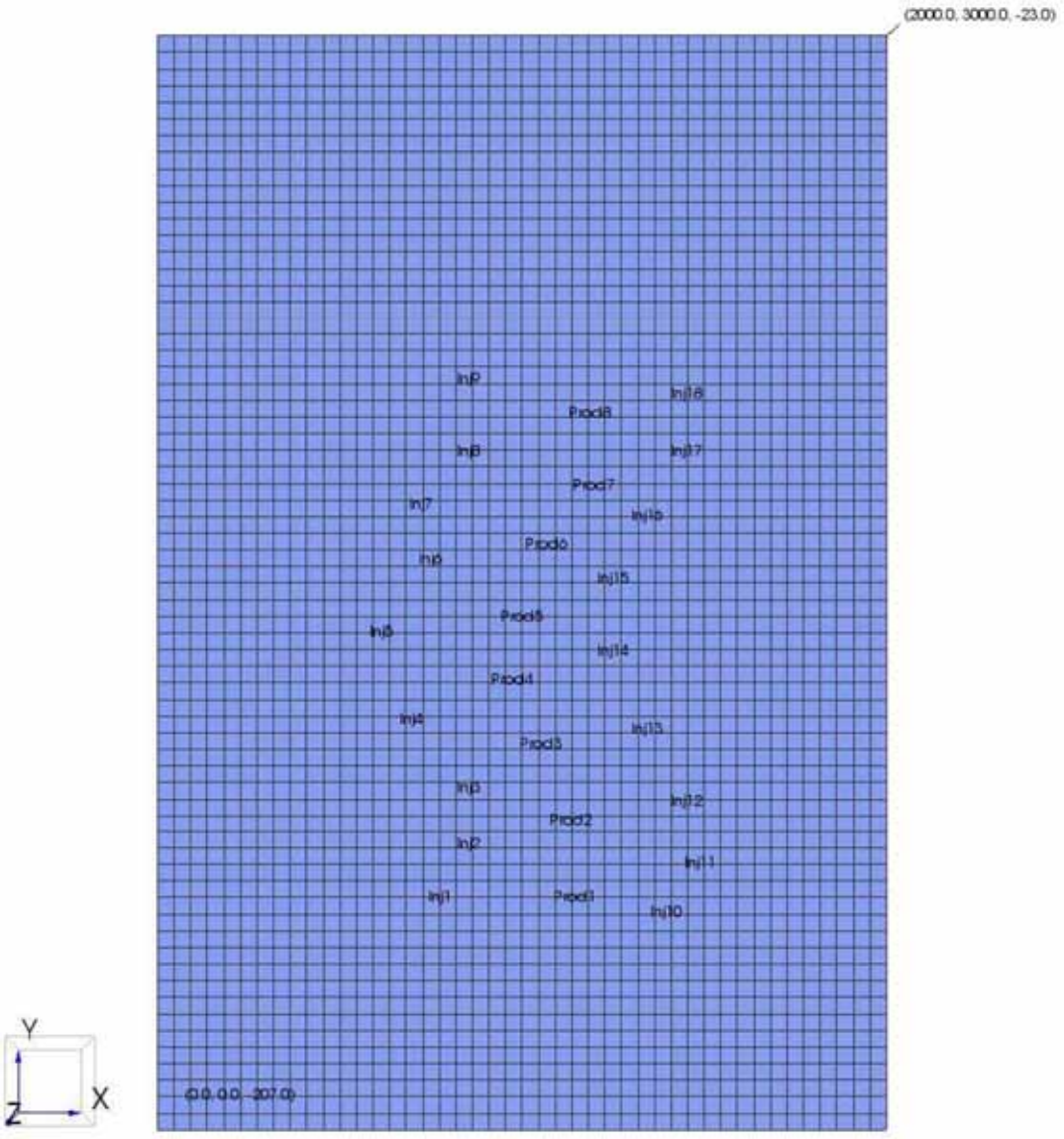

Figure 2: Hypothetical well layout used in GSHE model.

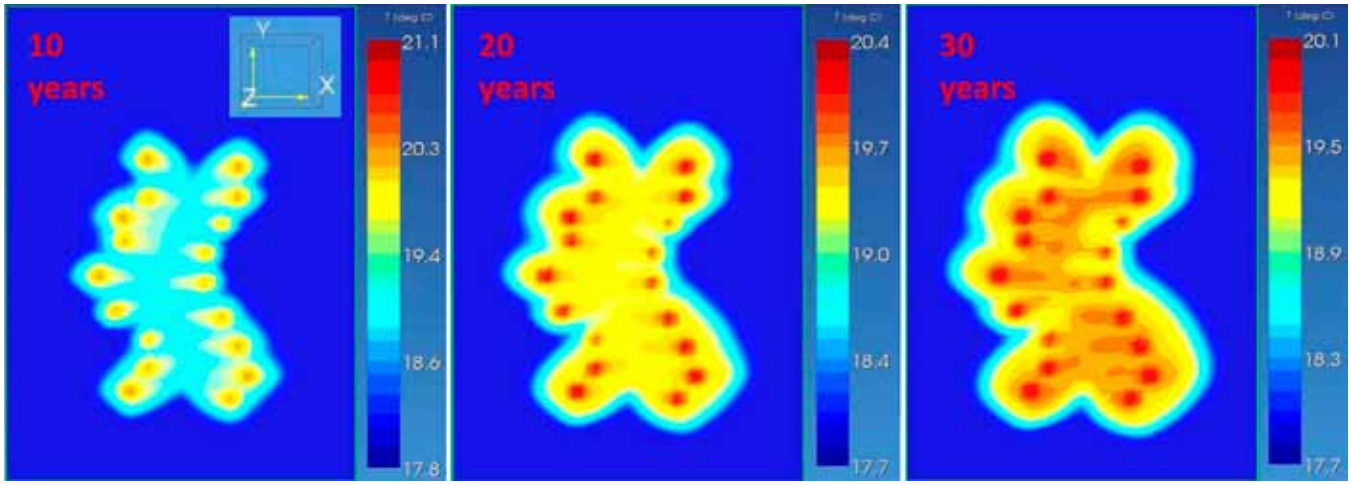

Figure 4. Temperature distribution in aquifer at a depth of 23 meters.

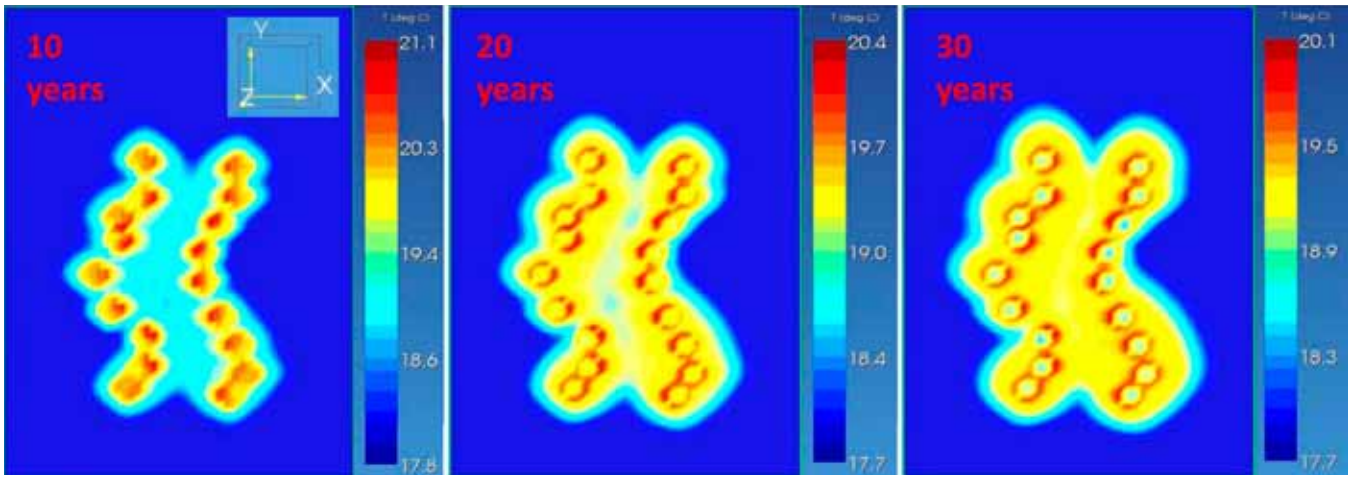

Figure 5. Temperature distribution in aquifer at a depth of 70 meters.

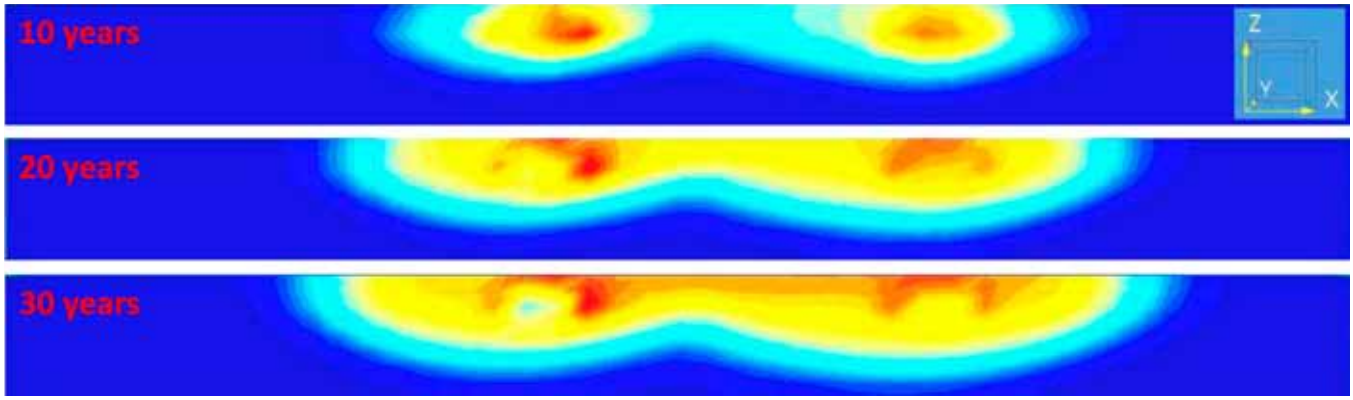

Figure 6. Temperature distribution in aquifer at a y-position of 700 meters (legends same as in Figures 3 and 4 for corresponding times).

given year (assuming the heat capacity of water is constant at 4,180 J/kg-°C). This is despite the fact that the amount of cool water injected during the heating season exceeds the amount of warm water injected during the cooling season by 0.8 megatonnes/yr. In other words, the temperature difference during the cooling season exceeds the temperature difference during the hating season. The estimated heat flow into the aquifer is illustrated in Figure 7.

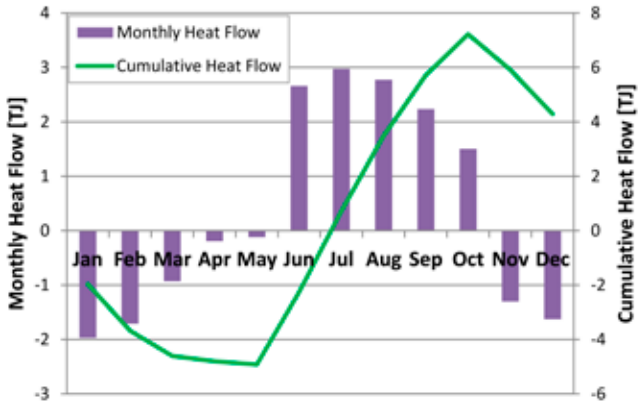

Figure 7. Estimated heat flow in the aquifer for a given year.

It should also be noted that there would actually be cold spots very close to the wells (inside of the hot spots) after 10, 20, and 30 years of operation, since each year ends during a heating season. This detail was most likely missed due to a relatively coarse discretization near the wells.

The evolution of temperature over time at the locations of the GSHE production wells is given in Figure 8. All eight production wells exhibit a similar increasing trend. This will ultimately change the temperature at which produced water can be reinjected as time progresses, a detail that will be incorporated into future modeling.

Additionally, all eight production wells exhibit periodic fluctuations in temperature associated with the switch between the heating and cooling seasons (i.e. these fluctuations have a period of 1 year). This periodic behavior is most pronounced in Producers 3 and 7, probably because these wells are positioned closest to the thermal plume coming from the injection wells in this particular well layout. An initial temperature drop can be observed in Producers 3 and 7, which is due to the fact that the simulation began in January, which is during a heating season.

CONCLUSIONS

Numerical simulation of mass and heat transport was performed to estimate how the implementation of an open loop GSHE for heating and cooling may impact groundwater temperatures. The results of this simulation for one hypothetical well layout and production plan indicate that the GSHE scenario considered would have a relatively small impact on groundwater temperatures. After 30 years of operation, groundwater temperatures in the region near GSHE wells experience local temperature increases of up to 2.3°C, but the thermal plume remains relatively close to the wells.

More detailed modeling which includes subsurface heterogeneity, the effects of the variability of production temperature on the reinjection temperature, and the influence of the operation of existing neighboring wells (injection and/or production) will be performed in the future to provide a more complete picture of possible impacts on groundwater temperatures. Sensitivity analysis will also be performed on flow properties, thermal properties, and natural groundwater flow rate.

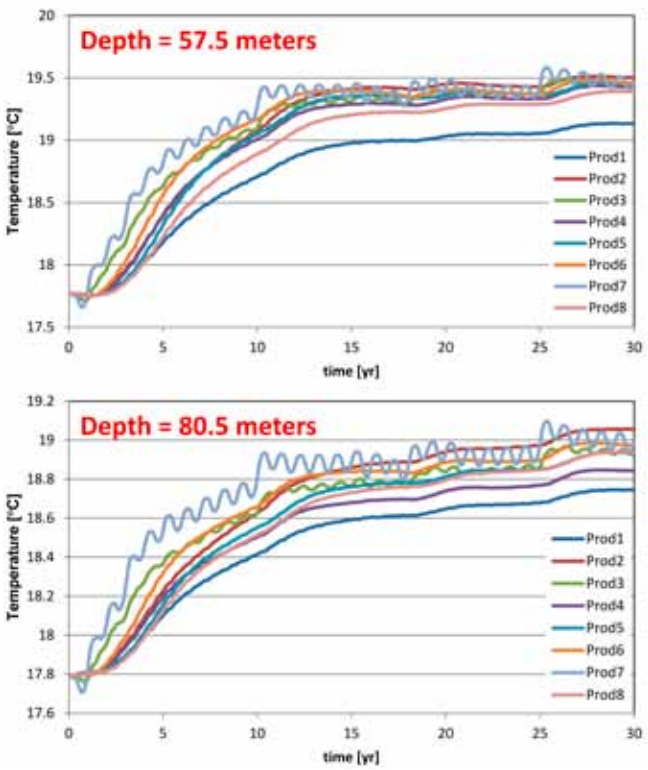

Figure 8. Evolution of temperature over time at different depths in GSHE production wells.

EDITOR'S NOTE

This paper was originally published in the 37th Stanford Geothermal Workshop proceedings and reprinted with permission from the Stanford Geothermal Program.

REFERENCES

Elson, Tom, 2011. "GSHE Modelling," Message to Roland N. Horne, E-mail (7 Dec 2011).

Google Maps. Web. <http://maps.google.com/>.

Haley & Aldrich, 2010. "Data Report: Ground Source Geothermal Evaluation - Stanford University, Stanford, California," Tech. no. 36590-702.

Luhdorff & Scalmanini Consulting Engineers, 2011. "Groundwater Utilization for Ground Source Heat Exchange: Stanford University," Tech. no. 11-1-089.

Meirovitz, Casey, 2011. "Tough2 Model Input," Message to the author, E-mail (8 Dec. 2011).

Pruess, Karsten, Curt Oldenburg, and George Moridis, 1999. TOUGH2, Computer software, Vers. 2, Earth Sciences Division, Lawrence Berkeley National Laboratory.

Stanford University Central Energy Plant Optimization Model (CEPOM), 2011. Patent pending.

Thunderhead Engineering, 2007. PetraSim, Computer software, Vers. 4.2.

MODELING THE EFFECTS OF DIRECT USE ON THE TAURANGA LOW-TEMPERATURE GEOTHERMAL SYSTEM, NEW ZEALAND

Sophie C. P. Pearson, GNS Science, Wairakei Research Centre, Taupo, New Zealand

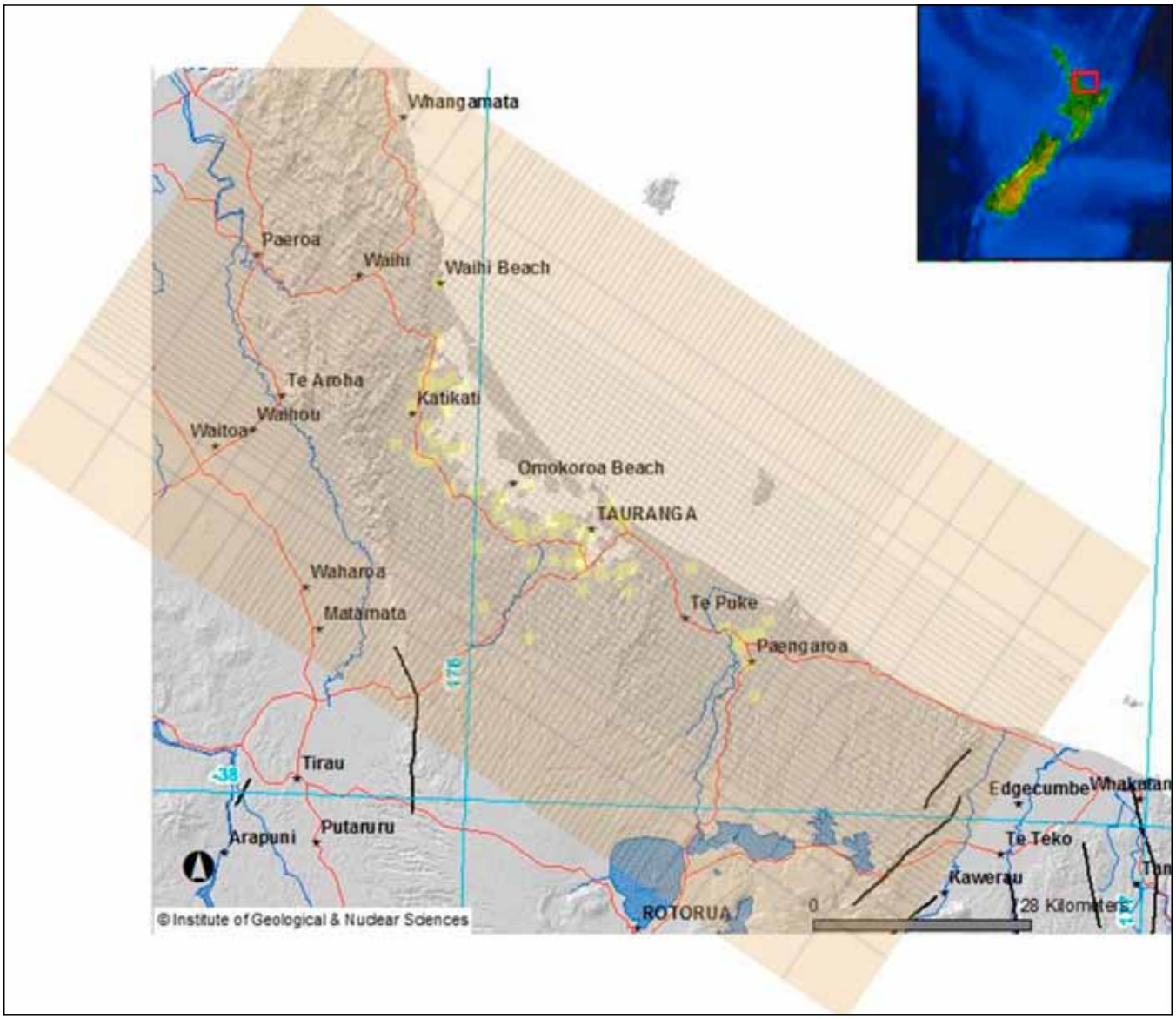

Figure 1. Location map of Tauranga geothermal field. The brown grid shows the model extent and dimensions. Yellow dots represent cells with well data. Black lines correspond to major faults. Inset map: Location of Tauranga within New Zealand.

ABSTRACT

Tauranga, on the north coast of the North Island of New Zealand, is the site of a fairly extensive low-temperature (60°C at 800 m) geothermal resource that is currently used for hot pools, swimming baths, domestic use, greenhouses and tropical fish growing. As the population of the area grows and interest in direct use of geothermal resources increases, the system comes under increasing demand. In this study, a TOUGH2 heat and fluid flow model of the Tauranga geothermal field is used to determine the extent of the system, and the possible effects of withdrawing hot fluid from the area.

The TOUGH2 model covers a 70 by 130 km area and extends to 2 km depth. Modeled temperatures matched measured well temperatures using surface heat flow rates to constrain the heat input at depth. The high temperature gradient observed in the top 500 m was replicated using a low thermal conductivity of 1.05 W/m°C in the shallow Tauranga Formation sediments. A good match could be obtained over the majority of the field using a homogeneous 2-layer model and two zones of basal heat influx. The model shows that heat flow is conductive to the northwest, but convective to the southeast. The geothermal system appears to be stable over long periods of time in its natural state.

When warm water is extracted, the pressure of the system re-equilibrates within a few months. However, there is a permanent decrease in temperature. After extraction has ended, the system takes hundreds of years for the temperature to return to its natural-state levels. Therefore it is important that these systems are carefully managed, and that modeling is carried out to ensure that they are not over-produced.

INTRODUCTION

Geothermal systems play a vital role as an energy source in New Zealand. 19% of total primary energy is geothermal, and 13% of electricity generation is from high-temperature geothermal sources (Ministry of Economic Development, 2011). Low temperature resources are particularly of increasing interest; in 2010 ~10 PJ of energy was used for industrial, commercial, agricultural and residential direct uses, an increase of 35% since 1990 (Ministry of Economic Development, 2011). It is therefore important to ensure that these systems are used and maintained in an effective and sustainable manner. TOUGH2 numerical modeling is often used to assess high-temperature geothermal systems (O'Sullivan et al., 2001), but here we apply it to the Tauranga low-temperature geothermal field to assess its energy potential and the effects of withdrawing hot fluid.

TAURANGA GEOTHERMAL FIELD

Tauranga is located on the north coast of the North Island of New Zealand (Figure 1). It is a city with approximately 120,000 people, making it the sixth largest urban center in New Zealand (Statistics New Zealand, 2012). It is bounded to the west by the Kaimai mountain range and to the east by the Pacific Ocean. The Tauranga area itself is relatively flat, other than Mount Maunganui (252 m) which is situated on the spit just north of Tauranga town (Figure 1).

Geologic Setting

Tauranga is located close to the subduction zone between the Pacific and Australasian plates. It is situated in the Tauranga Basin, a tensional graben formed about 2-3 million years ago (Davis & Healy, 1993). The basin sits within the Coromandel Volcanic Zone, a north-northwest trending zone that was highly active in the Miocene-Pliocene (Briggs et al., 2005). Volcanism commenced at ~18 Ma (Adams et al., 1994) but shifted to the Taupo Volcanic Zone between 1.9 and 1.55 Ma (Briggs et al., 2005). During this time at least 21 dacite-rhyolite domes or dome complexes and three defined ignimbrite formations were emplaced (Briggs et al., 2005). The remnant heat from these domes is thought to be the source of the warm water system at Tauranga (Reyes, 2008).

In a large part of the Tauranga area, the volcanics have been overlain by relatively young sediments. The Minden rhyolite domes remain some of the most dominant landforms, but these have been overlain inland by sediments dated at ~6.5 ka (Davis & Healy, 1993). Tidal sediments are somewhat younger, between 3.4 and 0.7 ka (Davis & Healy, 1993). Sediments thicken seawards (Simpson and Stewart 1987), reaching a thickness of 300 m under Matakana Island, but disappearing to the west of our study area (White et al., 2009). There are major faults to the south and west of our study area, but none within it (Figure 1) (Briggs et al., 2005).

Geothermal System

The Tauranga geothermal field is a significant low-enthalpy resource. There are a number of springs with water at between 22 and 39˚C, and temperatures of up to 60˚C have been measured in wells drilled to 800 m depth (White et al., 2009). These low-enthalpy fluids are used primarily for bathing, but also for domestic use, greenhouses and tropical fish growing (White, 2009). Tauranga is a popular tourist destination and hot pools and commercial swimming pools are found throughout the area, while Highway Fisheries in Papamoa, to the southeast of Tauranga city, is a major grower of ornamental and tropical fish. Therefore the geothermal field plays a significant role for the area, and its long-term stability and further potential are of interest to the region's inhabitants and authorities.

TOUGH2 SIMULATION

We used the Petrasim interface to TOUGH2 to create a numerical model of heat and fluid transfer in the Tauranga area. TOUGH2 simulates multicomponent, multiphase flow in porous media. Full details can be found in Pruess (1991).

The Model

We created a model to encompass the entire Tauranga area and some distance beyond (Figure 1). It covers 70 km by 130 km and extends down to 2 km depth. It is orientated to the northwest to fit the geographical extension of the field and to cover the locations of warm-water wells (Figure 1). Over the warm water area the spacing is 1 km by 1 km, but beyond this it has a spacing of up to 10 km by 10 km to ensure that the warm-water area of interest in the center is not affected by the boundary conditions (Figure 1). The model comprises two rock types: sediments overlying volcanics. Initially the sediments were 150 m thick throughout, but later a more realistic stratigraphy was added where the contact dipped eastward so that the sediment thickness was 50 m to the west of the model but 300 m to the east (Figure 2).

The model was run with fairly simple initial conditions for two million years, to represent the age of the Tauranga Basin (Davis & Healy, 1993). Initially the interior and boundaries of the model were set at atmospheric pressure (101 kPa) and mean annual air temperature (12˚C) (NIWA, 2011). It was fully water saturated but the uppermost layer was 100% air to represent the atmosphere (Figure 2) and had a very large volume so that the atmospheric conditions were fixed. This allowed recharge into the system to be simulated at realistic rates. Recharge was injected into the second layer at 129 mm/yr (Figure 2) to simulate 10% of the mean annual rainfall (NIWA, 2011). Vertical boundaries were set as no-flow. As geochemistry suggests that there is minimal flow of geothermal fluids from depth (Reyes, 2008), heat was input into the base of the model at varying rates until an optimal fit was found between model temperatures and measured ones.

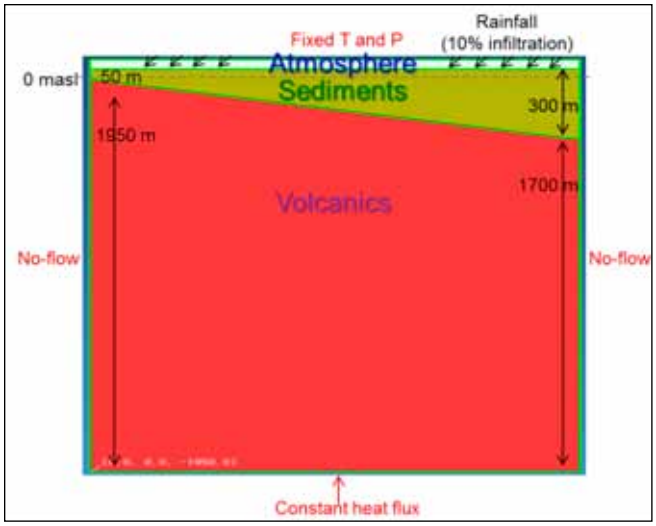

Figure 2. Cross-section of model showing stratigraphy and boundary conditions.

Constraints

A number of modeling constraints have been measured in or near the Tauranga area. Well temperatures were used as the primary constraint on the model. Geochemistry was used as a guide for boundary conditions. Basal heat flux, permeability and thermal conductivity were based on surface measurements but were varied to minimize the misfit between modeled and measured data. Density, specific heat capacity and porosity were set at measured/typical values.

Well Temperatures

The Tauranga area has been drilled extensively for groundwater studies, providing lithological and temperature information (White et al., 2009). More than 150 wells tap warm groundwater in 500 km^2 area around Tauranga (Simpson, 1987). Between 1960 and 2005 the temperature was measured in 73 wells. In 17 of them temperature profiles were recorded with depth, while the rest were measured at a single depth. The measurements were recorded at between 149 and -738 masl, from the surface to 752 m depth. Temperatures varied between 12 and 56˚C, with the majority at between 20 and 40˚C (White et al., 2009). In general deeper measurements were hotter (Figure 3). These well temperatures were used as the primary constraint for the TOUGH2 model. Other data in the area is also in agreement, with temperatures generally 35-45˚C at 600 m, but sometimes over 55˚C (Simpson, 1987).

Geochemistry

Geothermometry from the nearby Hauraki Fault suggests that temperatures are up to 160˚C (Reyes, 2008). Geochemical analysis shows that geothermal fluids in the Tauranga area are mainly heated groundwater with minor seawater in the north and minor magmatic volatiles in the south nearest to the Taupo Volcanic Zone (Reyes, 2008). Seawater intrusions have been noted around Mt Maunganui (Simpson & Stewart, 1987), although they are now thought to be at minimal levels (White, 2005).

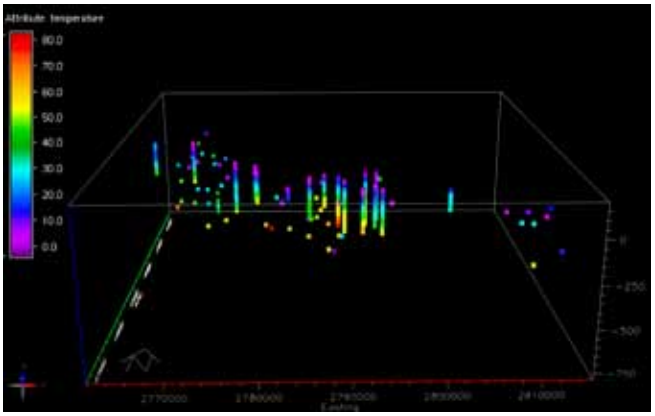

Figure 3. Temperature measurements from groundwater wells in Tauranga (White, Meilhac, et al. 2009) were used as the primary modeling constraint.

HEAT FLUX

Surface heat flux has been measured across the Tauranga area a number of times. As basal heat flux is a major variable in the model but is unconstrained, we used the surface heat flux as an initial guess for the basal flux rather than as an output of the model.

Average heat flow over the Tauranga area is measured as 88 ± 16 mW/m^2 (Simpson, 1987). In several distinct areas (Maketu, Mt Maunganui and around Tauranga Harbour edge) heat flow is above 120 mW/m^2, up to 336 mW/m^2. At one site a heat flow of 55 mW/m^2 was measured, but just 8 km to the southeast a heat flux as high as 200 mW/m^2 was recorded (Studt & Thompson, 1969). In the nearby Hauraki rift zone surface heat flux has been measured at between 80 and 90 mW/m^2 (Reyes, 2008). This means that there is considerable variability in the surface heat flux over relatively small areas. To prevent the model from becoming complicated beyond the level that the information can support, the average of 88 mW/m^2 was used across the base of the whole model initially and varied to refine the fit of the model temperatures to measured data.

Permeability

Permeability is difficult to constrain, but some work has been done in the Tauranga area. Outcrops show that volcanic rocks exhibit variable permeability and are fractured, allowing them to transmit fluid but not freely (Simpson, 1987). In general, the shallow groundwater system is fed by recharge in sediments while the deeper system contains considerably older fluids and is only recharged slowly by vertical seepage (Petch & Marshall, 1988).

In the Tauranga group sediments, permeability estimates in the Hamilton area (100 km away) range from 5 x 10^{-13} m^2 in the silts and sands to 9 x 10^{-12} m^2 in the coarse sands (Petch & Marshall, 1988). Bulk permeability is up to 8 x 10^{-11} m^2 (Heu, 1985). As sediments are typically less permeable than this (Bear, 1972) and the layer is thought to be a confining cap (Simpson, 1987), the upper value of 5 x 10_{-13} m^2 was used.

Estimates of shallow permeability in volcanic rocks in Auckland (200 km away) are similar to those for Tauranga sediments. They range from 2 x 10^{-13} to 8 x 10^{-11} m^2 for volcanic rocks that have little or no scoria, and from 8 x 10^{-12} to 8 x 10^{-10} m^2 for volcanic rocks with significant amounts of scoria (Harding et al., 2010). The bulk permeability is likely to be significantly lower than this (O'Sullivan, personal communication, December 2010) because our model extends to some depth (Ingebritsen & Scholl, 1993). Harding et al. (2010) did not find any evidence of significant horizontal/vertical anisotropy.

Other rock properties

A number of measurements have been made in the Tauranga area that provides extremely useful information for heat and fluid flow models. For the Tauranga Formation sediments, the thermal conductivity has been measured at 1.05 W/m°C (Simpson, 1987). This was therefore used in the model, although other values were also tried. Typical values of 2,500 kg/m^3 and 0.1 were used for the rock density and porosity respectively. For the volcanic rocks in the Tauranga area, more measurements have been made and so a larger range of properties have been constrained. Taking an average of all of these values gives a density of 1,890 kg/m^3, a porosity of 0.42 and a thermal conductivity of 1.26 ± 0.05 W/m°C (Simpson, 1987). These were the values used in the TOUGH2 modeling.

Results

Modeling shows that with a fairly simple model of two rock layers and just two different zones of heat influx, a good match can be obtained to most of the well data (Figure 4). In the shallow sediments, a permeability of 5 x 10^{-13} m^2 provides the best match; lower permeability results in the model wells being slightly too cold. However, the model appears to be fairly insensitive to this parameter. In the volcanic rocks, permeability of more than 5 x 10^{-16} m^2 results in convection throughout the system. This would result in fairly large variability in well temperatures that is not observed, particularly in the northwest. Therefore a permeability slightly less than that suggested by the literature is required to match well temperatures with model data.

As the temperature of the field is fairly low, conduction is a major source of heat transfer. This means that the basal heat flux is very important. The average value of 88 mW/m^2 (Simpson, 1987) gives a good match to well data in the northwest of the model, but fluids in the southeast wells are generally hotter than model temperatures (Figure 5a). With a heat flux of 120 mW/m^2 to the southeast as suggested by surface measurements, the match is greatly improved (Figure 5b). Modeling suggests that this results in conduction to the northwest, but some convection to the southeast.

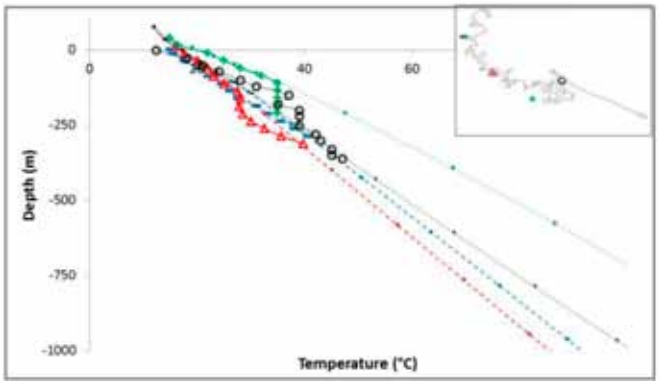

Figure 4. Match between measured (solid lines, large symbols) and modeled (dashed lines) data. The inset map shows the locations of the wells within Tauranga.

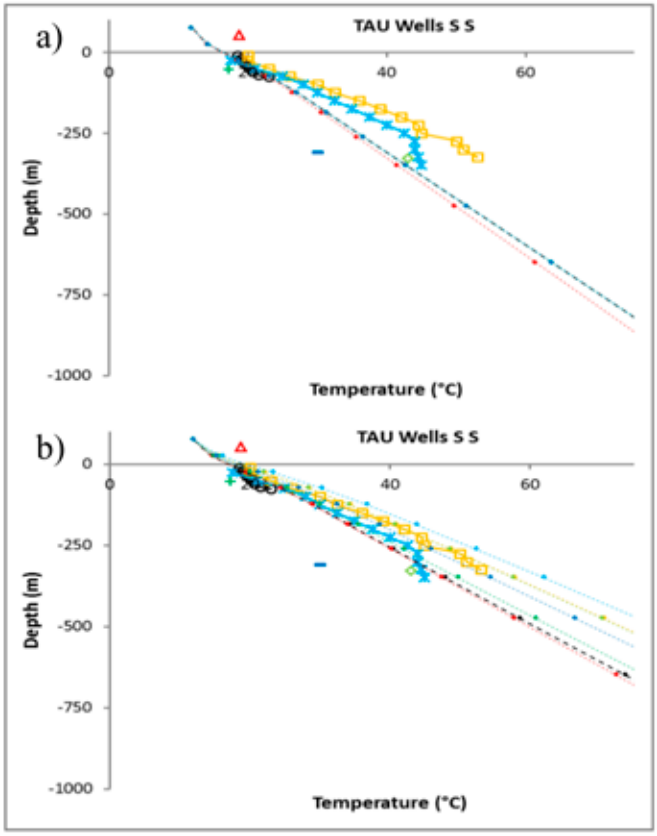

Figure 5. Model results to the southeast with varying basal heat flux. Dashed lines represent model results; solid lines and large symbols represent measured well data. a) Uniform heat injection of 88 mW/m^2. b) Heat injection of 88 mW/m^2 to the northwest and 120 mW/m2 to the southeast.

The model shows that the system is fairly sensitive to the thermal conductivity of the rock. Measured thermal conductivities are relatively low (Simpson, 1987), and these provide the best match to the data. With a higher thermal conductivity, the temperature does not increase quickly enough with depth. With a lower thermal conductivity, the shallow rock reaches very high temperatures. Therefore the measured thermal conductivities of 1.05 W/m°C in the sediments and 1.26 W/m°C in the volcanics appear to be fairly widespread within the system. In the sediments there is an unusually high thermal gradient of ~120°C/km in most of

the field which can be explained by this low thermal conductivity.

Although the well data did not include any colder areas to the south or west, the well to the north allows the northern boundary of the geothermal system to be identified to within 100 m (Figure 6), as northwest of Katikati but southeast of Waihi Beach (Figure 1). Adding more data to the south and west would allow the full extent of the geothermal field to be determined, important for understanding the system and its potential capacity. Changing the contact between the volcanics and sediments from horizontal to the more realistic dipping to the east does not affect many of the results, but does improve the fit in some cases.

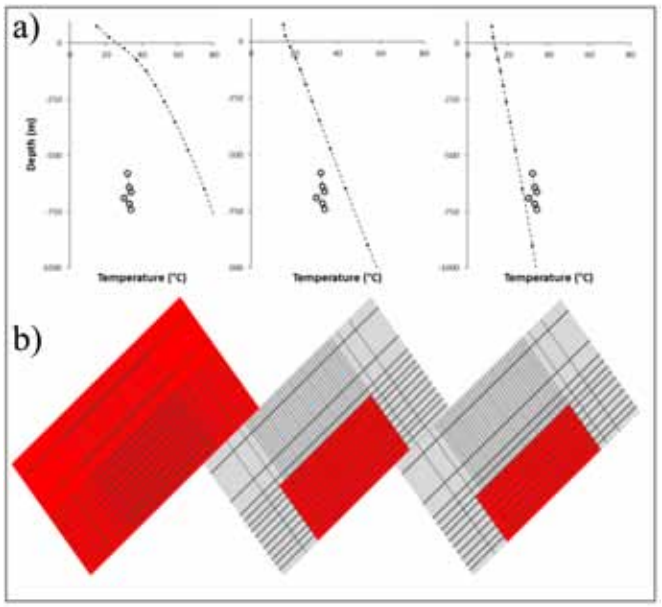

Figure 6a.) Model results (dashed lines) compared to data (symbols) in the furthest north well at Waihi Beach (Figure 1). Reducing the area of heat input from left to right (b), significantly improves the fit, allowing the northern extent of the system to be determined to within 100 m.

Modeling allows the energy and fluxes contained within the Tauranga system to be determined. It suggests a total energy of 228 MW within the system, but spread over 2,360 km^2. The average fluid flux is just 2.6 x 10^{-9} kg/m^2s at the surface over the area of heat input. The maximum fluid flux is 1.5 x 10^{-6} kg/m^2s, with a heat flux of 595 mW/m^2. This maximum heat flux is slightly higher than surface measurements, but within an order of magnitude. These model results suggest that there is significant energy potential within the system, but that it is widely distributed throughout the area.

Calculating errors throughout the model allows us to identify the areas that are most poorly represented. The average error is 27%, with 70% of errors less than 25% (Figure 7). This is acceptable, particularly as many measurements are single values recorded in open wells during different times of year and they are fairly small numbers so errors are proportionally larger. However, in the center of the field (W2018) there is an error of 186% (Figure 7), possibly due to topographic effects, localized variations in depth to the heat source, rock properties or measurement error.

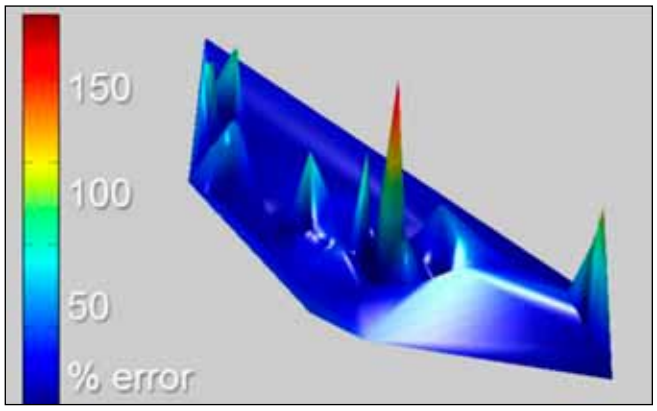

Figure 7. Plot of misfit between model temperatures and well measurements.

PRODUCTION

As there is a significant amount of energy within the Tauranga geothermal system but it is spread over a wide area, over-utilization could definitely become a problem. Therefore we used the TOUGH2 model to study the effects of withdrawing fluid. We started by simulating a production well in the center of the model for 100 years. The depths of production were 75 m (near the surface), 125 m (at the contact between volcanics and sediments), 350 m (within the volcanics) and 650 m (within the volcanics near the depth of the deepest well). Rates varied from 4 to 40 kg/s in the one cell, so from 4 x 10^{-6} to 4 x 10^{-5} kg/m^2s. This is up to an order of magnitude greater than the maximum modeled fluid flux and four orders of magnitude greater than the average.

Modeling a medium production rate at different depths shows that this should be sustainable (Figure 8). For production at 8 kg/s (8 x 10^{-6} kg/m^2s) with shallow production, the temperature decreases steadily over 100 years but the pressure is only minimally affected (Figure 8). In contrast, for deep production the temperature remains stable but the pressure decreases. The pressure decrease is very rapid however; after 2 months the system has restabilized but at a lower value (Figure 8). This suggests that shallow production, from within the sediments, would cause the system to continually cool, whereas deeper production from within the volcanics could affect surface features as the pressure drops, but would then be more stable over the long term.

For the volcanic-sediment interface (125 m depth), a range of production rates shows that, as expected, the higher the production rate the greater the decrease in temperature and pressure (Figure 9). Again, the pressure restabilizes after a few months but at a lower level, while the temperature decreases steadily by as much as 10°C for the highest withdrawal rate, and by at least 2°C for a withdrawal rate on the same order of magnitude as the maximum modeled. This is a decrease of between 6 and 30%.

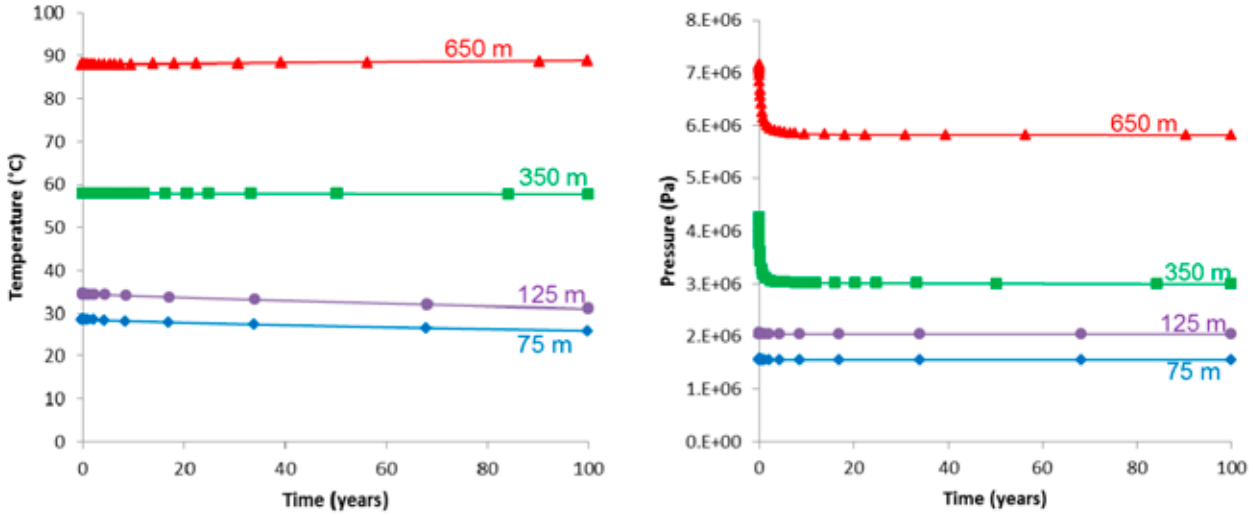

Figure 8. The effects of withdrawing fluid at 8 kg/s over a 1 km² area. Numbers represent the depth of production.

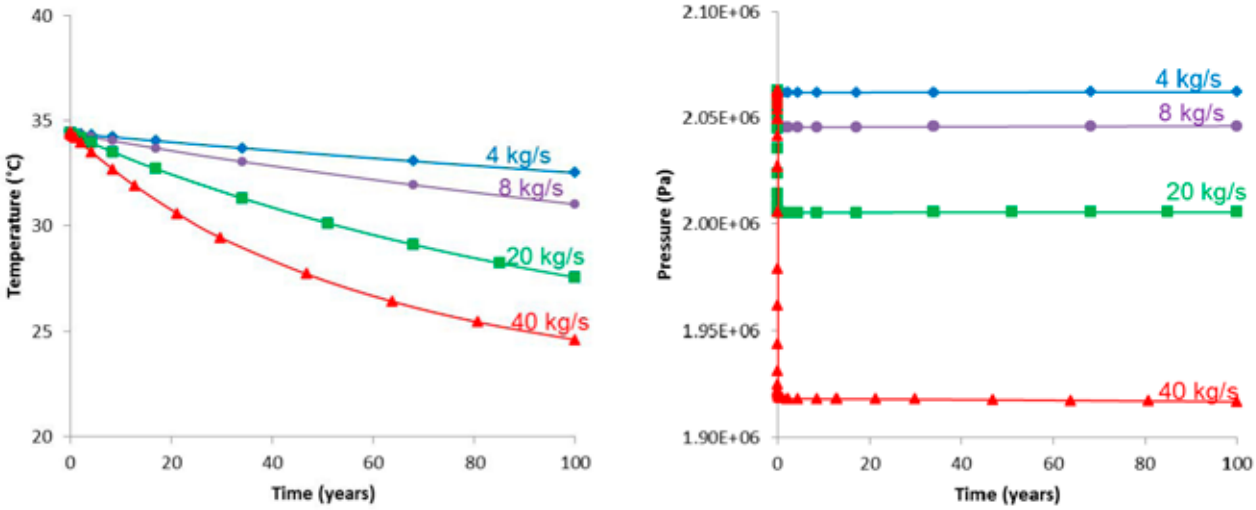

Figure 9. Effects of withdrawing fluid from the sediment-volcanic interface. Numbers represent the production rate over a 1 km² area.

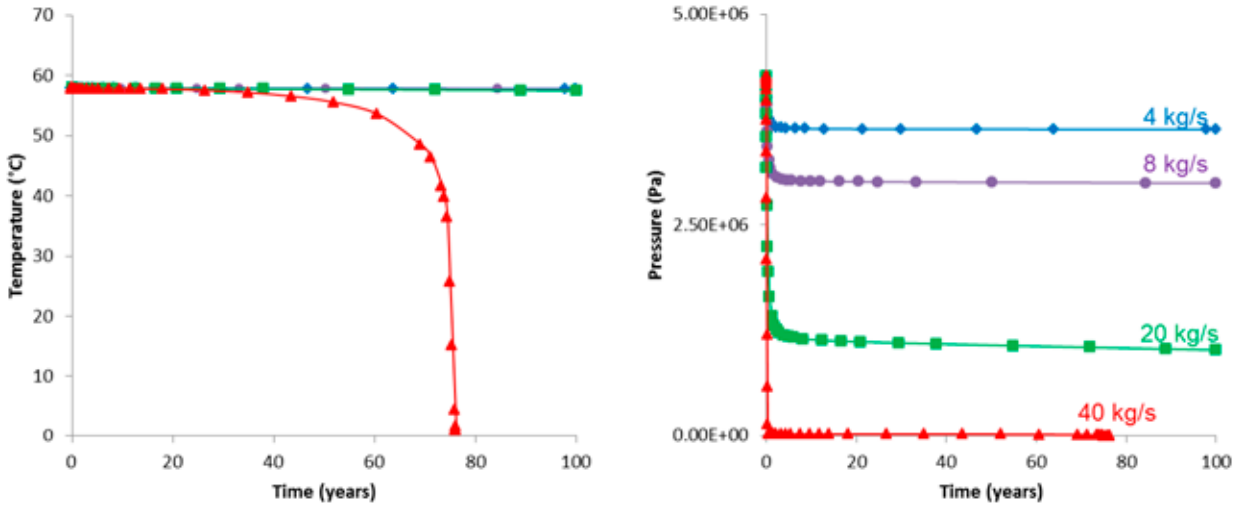

Figure 10. Effect of withdrawing fluid at 350 m depth. Numbers represent withdrawal rates. For the highest withdrawal rate, the system dies after less than 80 years.

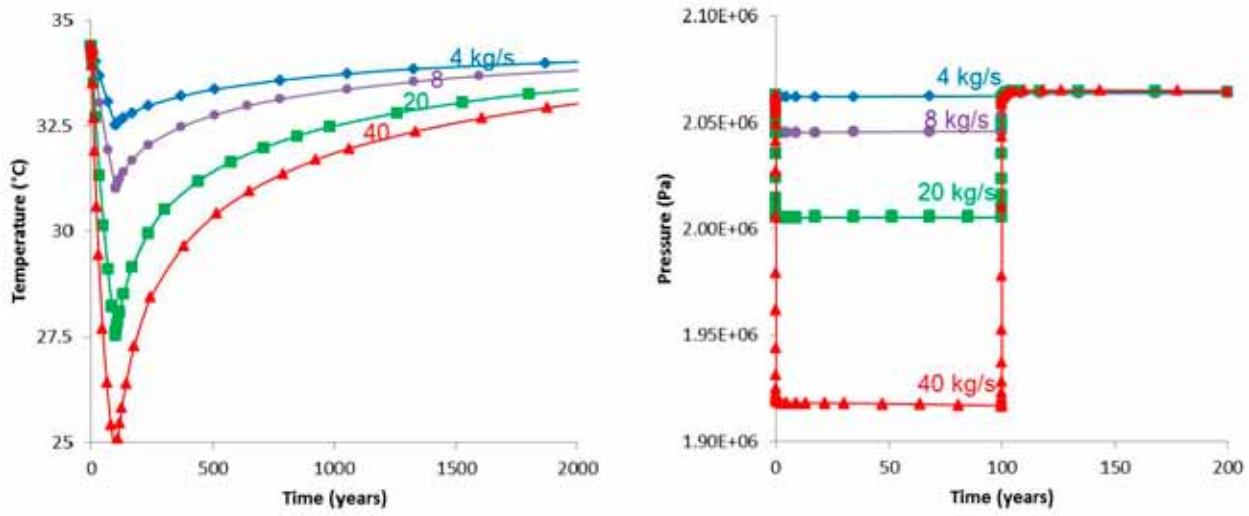

Figure 11. Simulated recovery of the system after production. Numbers show the rates of production at 125 m depth. Withdrawal was modeled for 100 years and was then turned off.

For the deeper wells, within the volcanics, the effect of high withdrawal rates can be even more severe. At 350 m depth, the temperature remains stable but the pressure drops significantly for rates of 4 – 20 kg/s (Figure 10). For 20 kg/s, the pressure decreases by more than half which would definitely affect surface features. At a withdrawal rate of 40 kg/s, the system essentially dies as it cools down and dries up (Figure 10). Therefore it is important to manage withdrawal from these types of systems, and to decide on the maximum induced variations that would be acceptable.

RECOVERY

Another important aspect of the system to understand is its recovery after withdrawal has ended. The model was therefore run for another 10,000 years after switching off the well. It shows that the system does recover, but very slowly (Figure 11); after 100 years less than 25% of the temperature loss has been recovered. After 1,000 years the temperature is half-way back to background levels, but it takes a full 10,000 years for the system to re-approach its natural state. However, the pressure again re-stabilizes after only two months, and at the original levels. This suggests that the Tauranga system is stable before, during and after production, but heat is essentially lost permanently, and it would take the system a very long time to recover from over-production.

CONCLUSIONS

The Tauranga geothermal field is a low-temperature system that contains ~225 MW over more than 2,300 km^2. Modeling allows the northern extent of the field to be determined, and shows that the low thermal conductivity measured in the Tauranga sediments is the best explanation for the relatively high thermal gradient measured in wells in the area. The heat flux was found to be the main constraint on the model, although a simple two-zone model with 88 mW/^{2} to the northwest and 120 mW/m^2 to the southeast results in a good match between measured and modeled temperatures. The average modeled fluid flux above the heat source is just 2.6 x 10^{-9} kg/m^{2}s, while the maximum fluid flux is 1.5 x 10^{-6} kg/m^{2}s with a maximum heat flux of 595 mW/m^2. This suggests that there is significant energy within the system, but that it is generally very diffuse and therefore only appropriate for direct use.

Modeling production scenarios shows that for rates twice that of the maximum modeled as naturally occurring within the system, shallow wells cause a constant decrease in temperature, while deep wells result in a rapid drop in pressure that then re-stabilizes at a lower level. For a withdrawal rate ten times modeled, production from the deep wells results in the entire system dying. Modeling recovery suggests that it is very slow, on the order of thousands of years. The pressure appears to be stable, but the effect of withdrawal on the temperature of the geothermal system is essentially permanent. Therefore it is vital that these systems are well managed to ensure that fluid withdrawal is sustainable.

FUTURE WORK

There are a number of steps that we hope to achieve to improve this model. Initially, the misfit between measured and modeled well temperature data needs to be addressed by varying topography, local rock properties and/or heat flux. There may also be more well data that can be included in the model, particularly to the southern and western extents of the currently modeled warm water area.

Having improved the model and recalibrated it, we hope to simulate more production scenarios. Well locations, depths and approved withdrawal amounts from the local authorities will allow us to assess current and future usage rates and their potential long-term effects. We will also model reinjection scenarios based on actual data. From this we will be able to deduce whether the system is cooling, and if currently approved rates are sustainable. We then hope to add some additional wells to see if the current system capacity can be increased for direct use.

EDITOR'S NOTE

This paper was originally published in the 37th Stanford Geothermal Workshop proceedings and reprinted with permission from the Stanford Geothermal Program.

REFERENCES

Adams, C. J., Graham, I. J., Seward D., and D. N. B. Skinner, 1994. "Geochronological and Geochemical Evolution of Late Cenozoic Volcanism in the Coromandel Peninsula, New Zealand." *New Zealand Journal of Geology and Geophysics*, 37, 359-379.

Bear, J., 1972. *Dynamics of Fluids in Porous Media*. New York, Dover Publications.

Briggs, R. M., Houghton, B. F., McWilliams, M., and C. J. N. Wilson, 2005. "40Ar/39Ar Ages of Silicic Volcanic Rocks in the Tauranga-Kaimai Area, New Zealand: Dating the Transition between Volcanism in the Coromandel Arc and the Taupo Volcanic Zone." *New Zealand Journal of Geology and Geophysics*, 48, 459-469.

Davis, R. A., and T. R. Healy, 1993. "Holocene Coastal Depositional Sequences on a Tectonically Active Setting: Southeastern Tauranga Harbour, New Zealand." *Sedimentary Geology*, 84, 57-69.

Harding, B. C., Pattle, A., Harris, M. G., and G. Twose, 2010. "Groundwater response to the dewatering of a volcanic vent." *Proceedings of IAEG Congress 2010*, Auckland, New Zealand.

Heu, A. S., 1985. "Weavers opencase hydrological investigation: Interim Report". *New Zealand State Coal Mines Geomechanics Report* 85/12.

Ingebritsen, S. E., and M. A. Scholl, 1993. "The hydrogeology of Kilauea volcano." *Geothermics* Volume 22, 255-270.

Ministry of Economic Development, 2011. *New Zealand Energy Data File*. Wellington, New Zealand: Energy Information and Modelling Group.

NIWA. The National Climate Database. 5 May 2011. http://cliflo.niwa.co.nz/pls/niwp/wgenf.genform1.

O'Sullivan, M. J., Pruess, K., and M. J. Lippmann, 2001. "State of the art of geothermal reservoir simulation." *Geothermics*, Volume 30, 395-429.

Petch, R. A., and T. W. Marshall, 1988. "Ground water resources of the Tauranga Group sediments in the Hamilton Basin, North Island, New Zealand." *Journal of Hydrology*, New Zealand, 27, 81-98.

Pruess, K., 1991. TOUGH2 - *A general purpose numerical simulator for multiphase fluid and heat flow*. Berkeley, CA: Lawrence Berkeley Laboratory.

Reyes, A. G., 2008. "Water-rock interaction in a low-enthalpy back-rift geothermal system, New Zealand." *Geothermal training programme*. Reykjavik, Iceland: United Nations University, 1-8.

Schofield, J. C., 1972. "Ground water of the Hamilton Lowland." *New Zealand Geological Survey Bulletin*, 89.

Simpson, B., 1987. "Heat flow measurements on the Bay of Plenty coast, New Zealand." *Journal of Volcanology and Geothermal Research*, 34, 25-33.

Simpson, B., and M. K. Stewart, 1987. "Geochemical and isotope identification of warm groundwaters in coastal basins near Tauranga, New Zealand." *Chemical Geology*, 67-77.

Statistics New Zealand. Estimated Subnational Population (TA,AU) by Age and Sex at 30 June 2006–11 (2011 boundaries). 12 January 2012. http://www.stats.govt.nz/tools_and_services/tools/TableBuilder/intercensal-population-estimates-tables.aspx (accessed January 12, 2012).

Studt, F. E., and G. E. K. Thompson, 1969. "Geothermal heat flow in the North Island of New Zealand." *New Zealand Journal of Geology and Geophysics*, 12, 673-683.

White, B., 2009. *An updated assessment of geothermal direct heat use in New Zealand*. New Zealand Geothermal Association.

White, P. A., 2005. *Future use of groundwater resources in the Bay of Plenty region*. Institute of Geological and Nuclear Sciences client report 2005/127.

White, P. A., Meilhac, C., Zemansky, G. and G. Kilgour, 2009. *Groundwater resource investigations of the Western Bay of Plenty area stage 1 - conceptual geological and hydrological models and preliminary allocation assessment*. Consultancy Report 2008/240, Wairakei: GNS Science.

THERMAL RESPONSE TESTING OF GEOTHERMAL WELLS FOR DOWNHOLE HEAT EXCHANGER APPLICATIONS

Andrew D. Chiasson, Geo-Heat Center, Oregon Institute of Technology, Klamath Falls, Oregon

ABSTRACT

Accurate prediction of transient subsurface heat transfer is important in sizing downhole heat exchangers (DHEs) and making predictions of their thermal output, but quantification of these processes has been difficult and elusive in practice. As such, current DHE design methods rely on empirical data and rules of thumb. The work described in this paper makes use of so-called in-situ thermal response testing, in conjunction with a newly-adapted analytical solution that describes the coupled conductive and advective heat transport relevant to DHEs. The complex heat transfers within the well bore are described by a lumped thermal resistance parameter. A parameter estimation technique is applied to thermal response test data at a site in southern Oregon to quantify the average rock thermal conductivity, apparent average linear groundwater velocity, and wellbore thermal resistance. An example is given on use of the method to make DHE temperature output predictions over time of operation for an actual heating application.

INTRODUCTION

Accurate design tools for downhole heat exchangers (DHEs) in geothermal applications have remained elusive. This dilemma exists for essentially two main reasons: (1) lack of an easy-to-apply mathematical model that adequately describes heat transfer parameters relevant to DHEs, and (2) lack of a field test procedure to measure parameters for mathematical models. These reasons are intimately related, and detailed mathematical models are not applicable in practice if their solutions contain parameters that cannot be easily quantified in the field.

DHEs are unique in that they are characterized by numerous simultaneous heat transfer processes, namely: conduction through rock, advection due to regional groundwater flow, and natural convection of groundwater in the well bore. The design process is further complicated by the thermal resistance imposed by the DHE geometric configuration (i.e., pipe size, arrangement of pipes in the well bore, well completion and cased interval, presence of a convection promoter, and fluid flow within the DHE) and transient thermal loading applied to the DHE. Each of these processes is difficult to quantify in practice, and consequently, current DHE design methods rely on empirical data and rules of thumb.

The work described in this paper makes use of the so-called in-situ thermal response test, in conjunction with a newly-adapted analytical solution to describe the coupled conductive and advective heat transport relevant to DHEs to facilitate their design and predict their output. A key element of this approach is that it allows complex heat transfer processes within the well bore to be lumped into a single thermal resistance term. The thermal response test procedure is similar to that commonly conducted on closed-loop, grouted vertical borehole heat exchangers for use in geothermal heat pump applications, where a constant heat rate is applied to a circulating fluid stream in the DHE, and the inlet and outlet temperatures are recorded. The average rock thermal conductivity, apparent average linear groundwater velocity, and wellbore thermal resistance are estimated using a parameter estimation technique in conjunction with the analytical solution and thermal response test data.

BACKGROUND AND THEORETICAL CONSIDERATIONS

Culver and Reistad (1978) developed a design approach for DHEs that was centered around a so-called mixing ratio which was used to model convection cells in DHE well bores. This mixing ratio expressed the amount of groundwater leaving the well bore in proportion to new groundwater entering the well bore, and was used in conjunction with Darcy's Law to predict DHE output to within 10-15%. The shortcoming of the Culver and Reistad (1978) method is that there is no way of predicting the mixing ratio except by experience.

Pan (1983) examined convection promotion in wells with DHEs for direct application and conducted several field experiments. The model of Culver and Reistad (1978) was applied, and Pan (1983) concluded that the mixing process of water in the well bore was not well understood.

More recently, Chiasson and Gill (2008) applied Kelvin's Line Source Solution to a field-tested DHE in Puna District, Hawaii. That solution introduced a thermal resistance term that essentially lumped all heat transfer processes in the well bore and skin into one parameter. The shortcoming with the Chiasson and Gill (2008) approach was that the Line Source Solution is applicable to heat conduction only, and thus the predicted thermal conductivity value combined conductive and advective heat transport in the aquifer.

The approach used in this present paper for DHE design and predictive output is an analytical solution to the advection-dispersion equation. The solution has been adapted to conductive-advective heat transport for use with borehole heat exchangers by Chiasson and O'Connell (2011). Details are provided in that paper, and are summarized below.

The governing partial differential equation describing mass transport in the subsurface with flowing groundwater is described by the advection-dispersion equation, which has been derived by Bear (1972) and Freeze and Cherry (1979) for contaminant transport. By applying the law of conservation of energy to a control volume, an equation for heat transport

can be derived and expressed in two-dimensional Cartesian coordinates. For a homogeneous medium with a uniform velocity and two-dimensional flow with the direction of flow parallel to the x-axis, the governing equation simplifies to:

$$D_L \frac{\partial^2 T}{\partial x^2} + D_T \frac{\partial^2 T}{\partial y^2} - v_x \frac{\partial T}{\partial x} = R \frac{\partial T}{\partial t} \quad (1)$$

where:

$$D_L = a_L v_x + D^* \ \ and \ \ D_T = a_T v_x + D^* \quad (2a,b)$$

A list of symbols is provided in the Nomenclature section at the end of this paper. The $a_L v_x$ and $a_T v_x$ terms are referred to as mechanical dispersion in the longitudinal and transverse directions. In the mass-heat transport analogy, the diffusion coefficient (D^*) is modeled as an effective thermal diffusivity given by:

$$D^* = \frac{k_{eff}}{\emptyset \rho_l c_l} \quad (3)$$

where k_{eff} is defined as $\emptyset kl + (1-\emptyset)ks$, which is a volume-weighted average thermal conductivity of the saturated water/rock matrix and is necessary to distinguish between the thermal conductivity and thermal capacity of the water and soil/rock to account for the fact that heat is stored and conducted through both the water and rock, but heat is only advected by the water. A retardation coefficient (R) is also necessary to adjust the advection and diffusion terms to account for the fact that heat is stored and conducted through both the water and rock, but heat is only advected by the water (Bear, 1972). This is given by:

$$R = 1 + \frac{(1-\emptyset)\rho_s c_s}{\emptyset \rho_l c_l} = \frac{(\rho c)_{eff}}{\emptyset \rho_l c_l} \quad (4)$$

Chiasson and O'Connell (2011) adapted a mass-transport solution to Equation 1 for a continuous injection or extraction of heat (located at the origin, $x = 0$, $y = 0$) into a two-dimensional flow field with uniform groundwater flow velocity (v_x) parallel to the x-axis. The solution assumes an infinite medium with initial temperature T_o, constant thermal conductivity and diffusivity, and with constant heat transfer rate. This solution also assumes that water flows uniformly at constant velocity along the entire borehole length. The boundary conditions are given by:

$$\lim_{r\to 0}\left(-r\frac{\partial T}{\partial r}\right) = \frac{q\prime}{2\pi k_{eff}} \ \ and \ \ T_{r=\infty} = T_o \quad (5)$$

The solution for ground temperature at time t and distance x and y from the origin, and adjusting for thermal retardation, is given by:

$$\Delta T(x,y,t) = \frac{q'}{4\pi(\rho c)_{eff}\left(\frac{D_L D_T}{R^2}\right)^{1/2}} e^{\frac{v_x x}{2D_L}} \left(\int_{t_D=0}^{t_D=\infty} \frac{e^{-u-B^2/(4u)}}{u} du \right) \quad (6)$$

Chiasson and O'Connell (2011) noted that

$$\int_{\bar{r}^2/4Fo}^{\infty} \frac{e^{-u-b^2/(4u)}}{u} du = W\left(\frac{\bar{r}^2}{4Fo}, b\right)$$

where $W(u,\beta)$ is known in well hydraulics as the leaky well function, and is extensively tabulated by Hantush (1956). Therefore, Equation 6 can be written as:

$$\Delta T(x,y,t) = \frac{q'}{4\pi(\rho c)_{eff}\left(\frac{D_L D_T}{R^2}\right)^{1/2}} e^{\frac{v_x x}{2D_L}} \cdot [W(0,B) - W(t_D,B)] \quad (7)$$

where t_D is a dimensionless form of time given by

$$\left(\frac{v_x}{R}\right)^2 t \Big/ 4\frac{D_L}{R} \quad \text{and } W(0,B) = 2K_0(B),$$

where K_0 is the modified Bessel function of the second kind of order *0*. The average borehole wall temperature can be determined by computing temperatures at locations around the borehole wall. Note that for negligible groundwater flow rates, Equation 7 reduces to

$$\Delta T(r,t,\theta) = \frac{q\prime}{4\pi k_{eff}} W\left(\frac{\bar{r}^2}{4Fo}, 0\right)$$

which is equivalent to Kelvin's infinite line source solution, since

$$W\left(\frac{\bar{r}^2}{4Fo}, 0\right) = W\left(\frac{\bar{r}^2}{4Fo}\right) = \int_{\bar{r}^2/4Fo}^{\infty} \frac{e^{-u}}{u} du$$

where $W(u)$ is known as the well function in well hydraulics.

The average fluid temperature in the DHE (T_f) is then related to the change in the average borehole wall temperature (T_b) through the use of a steady-state borehole thermal resistance per unit length (R'_b):

$$T_f = \Delta T_b + q' \cdot R'_b + T_g \quad (8)$$

METHODOLOGY

Thermal Response Field Testing

A thermal response test was conducted at a residence in Klamath Falls, Oregon on a well that was used directly for space and domestic hot water heating. The DHE configuration consisted of a double PEX u-tube. The well was completed

with an was 8-inch (203-mm) diameter casing, approximately 30 ft (9 m) in length, and the well bore depth was recorded on the drilling log as 240 ft (73 m). The static water level in the well was recorded at 100 ft (30.5 m) below grade, giving a submerged length of DHE of approximately 140 ft (42.7 m). The well was completed in a basaltic aquifer.

The thermal response test was conducted using the portable apparatus shown in Figure 1. The undisturbed groundwater temperature was taken as the equilibrated water temperature circulating in the DHE under no thermal load. This temperature was measured at 140˚F (60˚C). A constant heat rate of 3400 W was applied to the fluid stream and the inlet and outlet temperatures to the DHE were recorded at 10-second interval using a Pace Scientific data logger. Raw test data results are shown graphically in Figure 2.

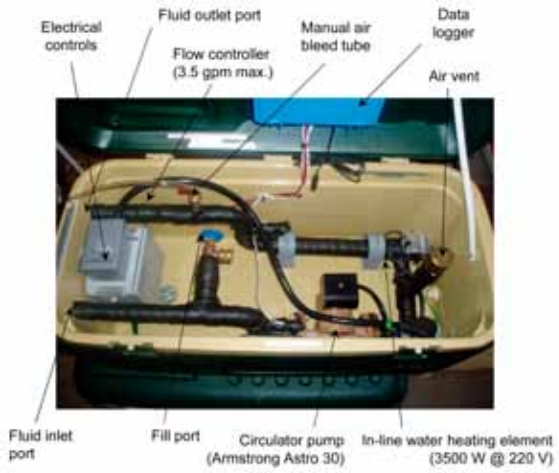

Figure 1: Photograph of portable field-testing apparatus.

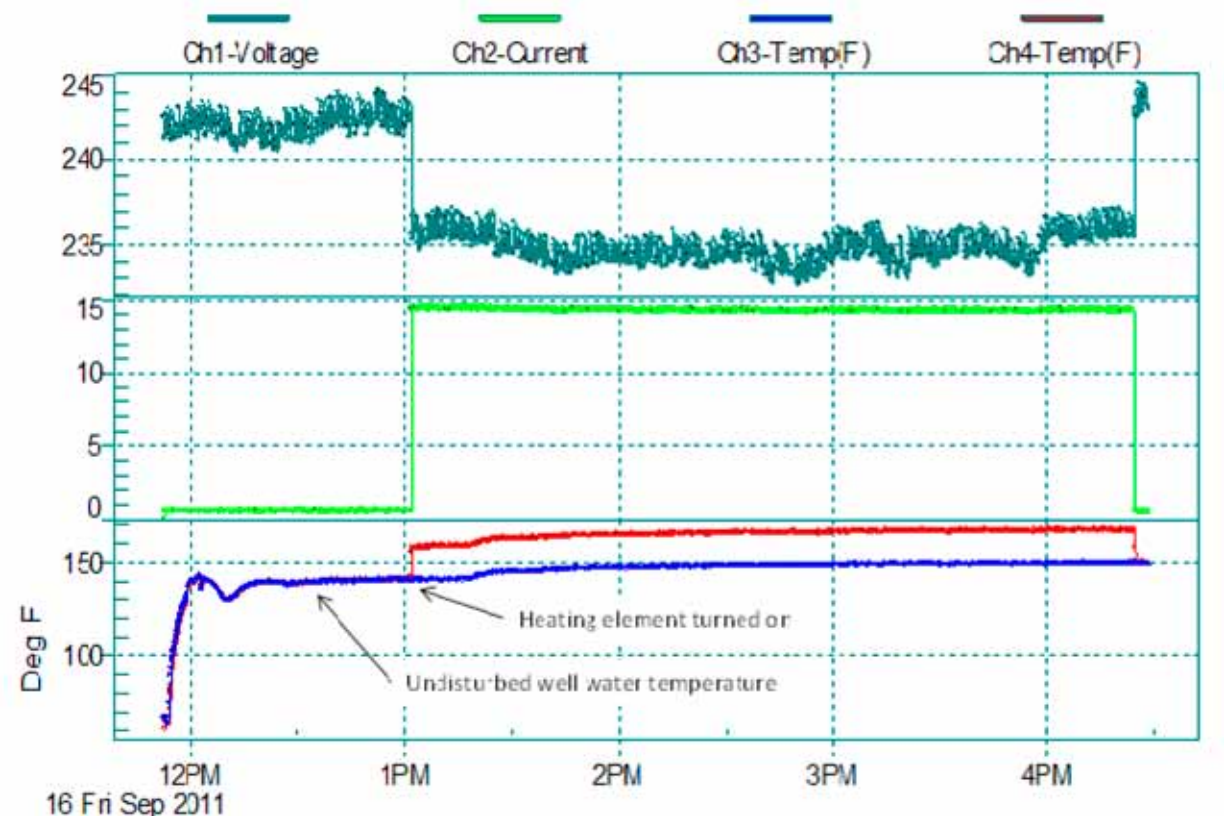

Figure 2: Graph of raw test data showing voltage current from the water heating element. Channel 3 is the water temperature leaving the DHE and Channel 4 is the water temperature entering the DHE. The data sampling rate was 10 seconds.

Application of the Mathematical Model with Parameter Estimation

Application of the analytical solution described above for heat transport in groundwater flow is cumbersome in practice because the groundwater velocity must be known, which requires knowledge of additional parameters, namely hydraulic conductivity, hydraulic gradient, and porosity. The solution using the mass-heat transport analogy requires knowledge of dispersivity, which is very difficult to measure in the field. Consequently, a parameter estimation technique is employed here, as discussed by Chiasson and O'Connell (2011) to determine unknown thermal and hydraulic properties that are relevant to DHE design. The parameters of most interest are: effective thermal conductivity, apparent average linear groundwater velocity, and the borehole thermal resistance. Of secondary interest are the longitudinal and transverse dynamic dispersivity values. Here, the average linear groundwater velocity is described as apparent, because it may not be a true value, given the complex nature of groundwater flow in geothermal aquifers. Therefore, the groundwater velocity may be more appropriately thought of as the effect of groundwater flow on the heat transfer characteristics of the DHE.

Parameter estimation involves minimizing the difference between experimentally obtained results and results predicted by a mathematical model by adjusting inputs to the model. As employed here, the results from the analytical solution are compared to thermal response test results. By systematically varying relevant parameters so that the minimum difference between the experimental results and the mathematical model is attained, a best estimate of the parameters of interest may be found. The relevant parameters varied were k_s, v_x, a_L, a_T, R'_b. An inherent issue with this approach is that the volumetric heat capacity must be estimated because inclusion of it in the optimization results in a non-unique solution. Fortunately, if the rock type is known, volumetric heat capacity does not vary significantly within rock types and does not significantly affect the optimization results.

The objective function for the optimization is the sum of the squared error (SSE) between the numerical model solution and the experimental results at each time of measurement, given by:

$$SSE = \sum_1^N \left(T_{experimental} - T_{model}\right)^2 \quad (9)$$

The optimization is performed with a nonlinear "downhill simplex" optimization technique of Nelder and Mead (1965).

RESULTS AND DISCUSSION

Thermal Response Test Results

Results of the mathematical optimization procedure are as follows:

- Average rock thermal conductivity: 1.2 Btu/hr-ft-F (2.1 W/m-K),
- Average linear groundwater velocity: 5,215 ft/yr (1,590 m/yr),
- Double PEX u-tube DHE thermal resistance (per unit length): 0.129 h-ft-F/Btu (0.0746 m-K/W).

The average rock thermal conductivity is typical of that of volcanic rocks, and the average linear groundwater velocity is of the same order of magnitude determined by tracer tests on the Klamath Falls aquifer. The DHE thermal resistance is similar to that determined in laboratory measurements by Claesson and Hellström (2000).

Crude Model Validation

Heat loss calculations were performed for the residence, and heat rates that the DHE must produce were determined as a function of outdoor air temperature. These heating loads, along with the optimized parameters from the thermal response test, were used as inputs to the analytical solution (Equation 7) to predict DHE output temperatures as a function of outdoor air temperature (Figure 3).

During the first cold spell of the 2011 Fall season in Klamath Falls, the overnight temperature dropped to approximately 35˚F (1.7˚C), and the measured temperature exiting the DHE was 112˚F. As seen from Figure 3, at an outdoor air temperature of 35˚F, the predicted DHE output temperature is 117˚F, which is in excellent agreement with the measured temperature. Obviously, more data are needed to fully validate the model, but initial results are promising.

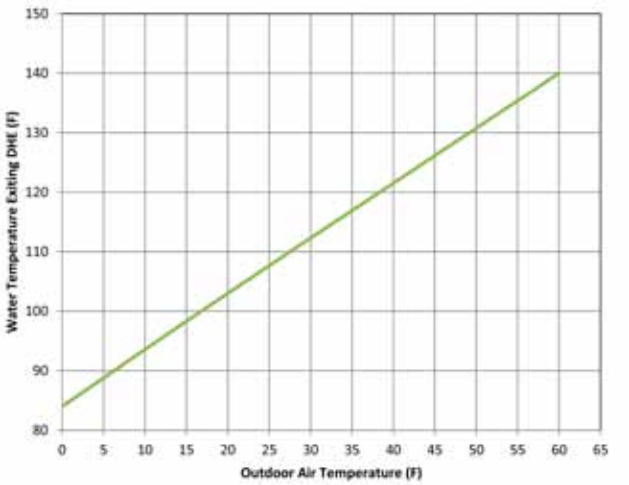

Figure 3: Graph of predicted DHE output temperature as a function of outdoor air temperature.

SUMMARY AND CONCLUSIONS

A useful and powerful method has been presented for determining the thermal output of DHEs in direct applications from geothermal wells. The method includes a readily applied mathematical model with parameters that can be easily measured in the field. With the use of a parameter estimation technique, the method has been roughly, initially validated for a residence in Klamath Falls, Oregon, but further validation of the model is needed.

EDITOR'S NOTE

This paper was originally published in the 37th Stanford Geothermal Workshop proceedings and reprinted with permission from the Stanford Geothermal Program.

REFERENCES

Bear, J., 1972. *Dynamics of Fluids in Porous Media*. New York: Dover Publications, Inc.

Chiasson, A.D. and Gill, A.T., 2008. "Field Performance Assessment of Downhole Heat Exchangers in Puna District, Hawaii," *Geothermal Resources Council Transactions*, Davis, CA, 32, 129-131.

Chiasson, A.D. and O'Connell, A., 2011. "New Analytical Solution for Sizing Vertical Borehole Ground Heat Exchangers in Environments with Significant Groundwater Flow: Parameter Estimation from Thermal Response Data," *HVAC&R Research*, American Society of Heating, Refrigerating, and Air-Conditioning Engineers, 17(6), 1000-1011.

GEO-HEAT CENTER
Oregon Institute of Technology
Klamath Falls, OR 97601-8801

Claesson, J. and Hellström, G., 2000. "Analytical Studies of the Influence or Regional Groundwater Flow on the Performance or Borehole Heat Exchangers," Terrastock 2000, *Proceedings of the 8th International Conference on Thermal Energy Storage*, 1, 195-200.

Culver, G. G. and Reistad, G. M., 1978. "Testing and Modeling of Downhole Heat Exchangers in Shallow Geothermal Systems," *Geothermal Resources Council Transactions*, Davis, CA, 2, 129-131.

Freeze, R.A. and Cherry, J.A., 1979. *Groundwater*. Englewood Cliffs, New Jersey: Prentice-Hall Inc.

Hantush, M.S., 1956. "Analysis of data from pumping tests in leaky aquifers". *Transactions of the American Geophysical Union*, 37, 702-714.

Nelder, J.A., and Mead, R., 1965. "A Simplex Method for Function Minimization". *Computer Journal*, 7 (1): 308-313

Pan, H., 1983. "Geothermal Downhole Heat Exchangers," Masters Thesis, Department Mechanical Engineering, University of Auckland, New Zealand.

NOMENCLATURE

a	dynamic dispersivity (ft [m])
B	$B = [(v_x^2 x^2)/(4D_L^2) + (v_x^2 y^2)/(4D_L D_T)]^{0.5}$
c	specific heat (Btu/lb·°F [J/kg·°C])
D	hydrodynamic dispersion coefficient (ft²/s [m²/s])
D^*	effective thermal diffusion coefficient (ft²/s [m2/s])
H	borehole depth (ft [m])
k	thermal conductivity (Btu/h·ft·°F [W/m·K])
K_0	modified Bessel function of the second kind of order 0
q'	ground thermal load per unit length of vertical bore (Btu/h/ft [W/m])
r	radial distance or radius (ft [m])
R	thermal retardation coefficient (--)
R'_b	borehole effective thermal resistance per unit length of bore (h-ft-°F/Btu [K-m/W])
t	time (s)
T	temperature (°F [°C])
v	average linear groundwater velocity (Ki/ϕ) (ft/s [m/s])
$W(u,\beta)$	Leaky well function (after Hantush, 1956) for arguments u and β
$W(u)$	Well function for argument u (equivalent to the exponential integral)
x, y	distance from origin in Cartesian coordinates

Greek Letters

α	thermal diffusivity (ft²/h [m²/s])
ϕ	porosity (--)
ρ	density (lb/ft³ [kg/m³])

Subscripts

avg	average
b	borehole
D	dimensionless
eff	effective
f	average fluid
g	undisturbed ground
gw	groundwater
in	inlet
l	liquid phase
L	longitudinal
out	outlet
s	solid phase
T	transverse
x,y	coordinate indices